

Constantly renewing glacial lakes in the Kyrgyz Range, northern Tien Shan

Mirlan Daiyrov¹, Chiyuki Narama²

¹Graduate School of Science and Technology, Niigata University, Niigata city, 950-2181, Japan

²Program of Field Research in the Environmental Sciences, Niigata University, Niigata city, 950-2181, Japan

5 *Correspondence to:* Mirlan Daiyrov (mirlan085@gmail.com)

Abstract. In the Kyrgyz Range of the northern Tien Shan, Central Asia, glacial lakes have been a focus of monitoring ~~because of due to the~~ increasing concern over glacial lake outburst floods (GLOFs) amid notable glacier recession. This study investigates (1) the historical evolution in ~~the numbers~~ and area of glacial lakes (each > 0.00045 km²) for ~~the period~~ 1968, 2000, and 2021, using Corona KH-4, Landsat 7, and Sentinel-2 imagery, and (2) the relationship between lake development and the evolution of glacier-moraine complexes (GMCs) containing buried ice. The number of glacial lakes doubled between 1968 and 2021, while the total area increased by 76% (0.80 to 1.42 km²). However, 190 out of 274 lakes present in 1968 had disappeared by 2000. Many new lakes ~~had~~ emerged by 2021, with one lake reappearing after a prior disappearance since 1968. Rapid lake formation was associated with a ~~3231~~ % reduction in glacier area over the past 50 years and the evolution of GMCs. The expansion and melting of buried ice ~~within of IDCs-GMCs~~ led to new surface depressions (thermokarst features) and subsequent lake formation, resulting in continuous glacial lake renewal. Thus, the continuous renewal of glacial lakes in the Kyrgyz Range results from the combined effects of glacier retreat, GMC expansion, and buried ice melt.

1 Introduction

It has been reported that the number of glacial lakes in ~~high-high~~ mountain regions of Asia is rapidly increasing (Zhang et al., 2023). In the Kyrgyz Range, located in the northern Tien Shan of ~~the~~ Kyrgyz Republic, hundreds of glacial lakes ~~have been are~~ identified by satellite data (Kattel et al., 2020; Daiyrov et al., 2022). Development of these lakes predominantly occurs on ~~glacier-glacier~~ moraine complexes (GMCs, Shatravin, 2007; Erokhin, 2011), which formed during glacier retreat after the Little Ice Age (LIA). GMCs, ~~is~~ also referred to as the ice-debris complexes (Bolch et al., 2018; Blöthe et al., 2021), ~~are-A GMC is-a~~ geomorphological units ~~that composed~~ ~~of buried ice and with debris moraine deposits, and are without~~ characterized by the absence of ~~clear distinct moraine ridges~~. Post-Little Ice Age ~~IA~~ climatic warming ~~has~~ induced geomorphological transformations ~~of in the recessional zones of glacier termini, where these moraine deposits, with glacier buried ice has become becoming isolated trapped beneath~~ ~~under debris as buried ice during glacier recession~~ (Maksimov, 1982; Maksimov and Osmonov, 1995; Erokhin et al., 2017). As ~~this~~ buried ice ~~has~~ melted, numerous glacial lakes formed on GMCs, sometimes in direct contact with their parent glaciers, but often as independent thermokarst lakes (Janský et al., 2008). Lakes directly connected to glacier ~~terminus-termini~~ typically exhibit faster expansion due to glacier recession, though ~~lakes~~ indirectly connected lakes ~~through debris-covered ice~~ can also enlarge ~~through debris-covered ice as that ice melts~~ (Daiyrov et al., 2018; 2022). Approximately 20% of these lakes are considered potentially hazardous (Janský et al., 2008, 2010).

Monitoring glacial lakes in the Kyrgyz Range is critical, as repeated GLOFs have caused severe damage (Erokhin et al., 2008, 2017; Kattel et al., 2020). Systematic research began in the 1960s following catastrophic GLOF events in ~~the~~ Kyrgyz Republic~~stan~~. In the central part of ~~the~~ Kyrgyz Range, at least 22 GLOF events have been recorded since 1952 (Erokhin, 2011; Zaginaev et al., 2016), including recent floods and debris flows such as Takyrtor glacial lake on 5 June 2009, Teztor glacial lake on 31 July 2012, Chelektor glacial lake on 12 August 2017, Akpai glacial lake on 2 August 2021 (Erokhin et al., 2017; Kattel et al., 2020; Daiyrov et al., 2022), and Takyrtor glacial lake on 27 June 2025. These events ~~have~~ damaged infrastructure, agricultural fields, and downstream settlements (Erokhin et al., 2017; Zaginaev et al., 2019), demonstrating the need for ongoing hazard assessment (Kattel et al., 2020; Daiyrov et al., 2022). Compared to the eastern Himalayas, where the glacial lakes have been expanding continuously for decades (Yamada et al., 1998; Komori et al., 2004; Nagai et al., 2017), glacial lakes in the northern Tien Shan, including the Kyrgyz Range, are smaller and more susceptible to unstable, short-term fluctuations due to geomorphological conditions, such as drainage ~~through~~ ice tunnels within GMCs (Daiyrov et al., 2018; Narama et al., 2018). Despite often being small, these lakes can pose significant hazards, especially ~~since because these~~ lakes described as “short-lived” (Narama et al., 2010, 2018; Daiyrov et al., 2018, 2022; Daiyrov and Narama, 2021) or “non-stationary” (Erokhin et al., 2017) ~~lakes~~ may form and drain in rapid succession, sometimes producing catastrophic GLOFs.

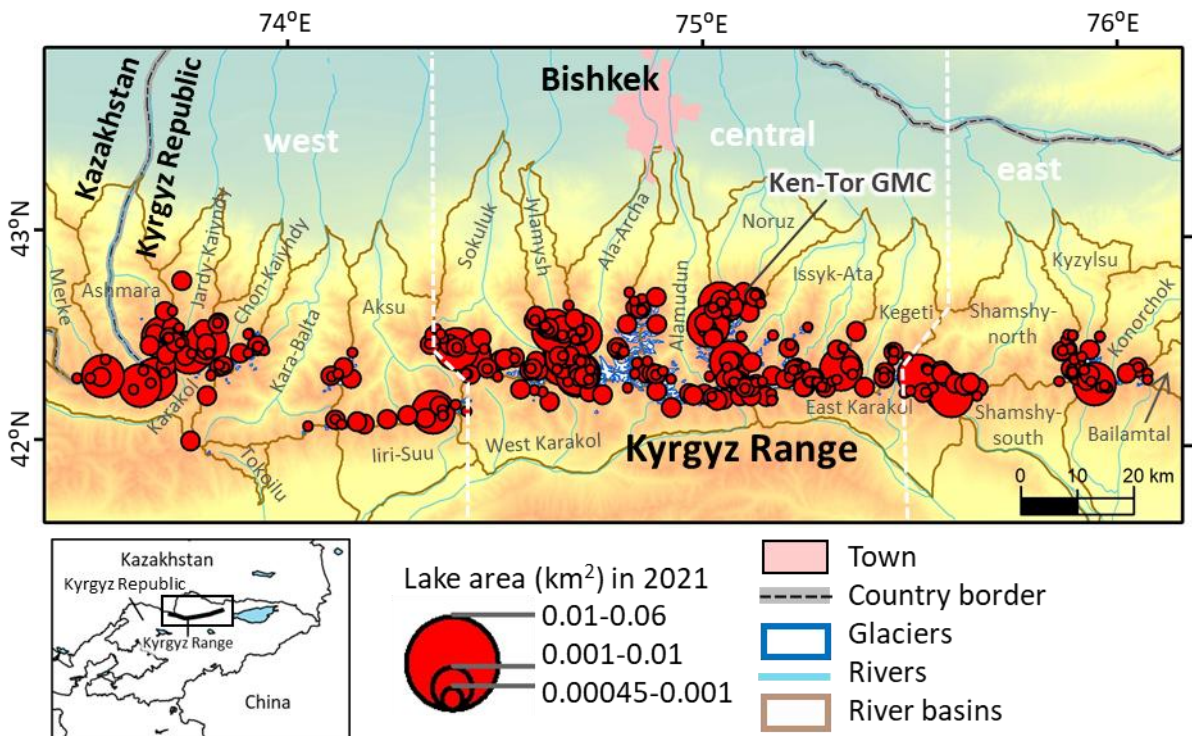
The increase in glacial lakes has been reported across High Mountain Asia (HMA). However, the processes of glacial lake formation and the factors ~~responsible for behind~~ GLOFs vary greatly from region to region. To accurately understand the relationship between glacial lake development and GLOFs, it is essential to ~~clarify~~ understand the distinctive ~~characteristics~~ features of each locality. In the Kyrgyz Range, Central Asia, previous studies ~~have~~ documented lake numbers and areas (Shatravin and Staviski, 1984; Jansky et al., 2006; Usubaliev and Erokhin, 2007; Erokhin, 2008; Falatkova et al., 2019; Daiyrov et al., 2022). Despite ~~these~~ observations, ~~of the number and area of glacial lakes~~, long-term changes in glacial lakes and the processes driving lake renewal in this region remain insufficiently documented. To understand the characteristics of ~~glacial lake~~ formation history ~~in glacial lakes~~ and to clarify the processes of rapid glacial lake renewal in the Kyrgyz Range, this study investigates (1) the historical evolution in ~~the~~ numbers and area of glacial lakes during 1968, 2000, and 2021, based on Corona KH-4, Landsat 7/ETM+, and Sentinel-2 imagery, and (2) the relationship between lake development and the evolution of glacier-moraine complexes (GMCs) containing buried ice. The latter relationship ~~was~~ ~~is~~ investigated through analysis of glacier area changes ~~derived due to from~~ ~~multivarious~~ remote sensing ~~datasets~~ imagery and ~~d~~ digital elevation models (DEMs) ~~for the study~~.

2 Study area

The study area is the Kyrgyz Range in the northern Tien Shan (Fig. 1), ~~where~~ with mountain ridges ranging from 2,500 to 4,900 m above sea level. The ~~central~~ northern flank ~~of the central part, which contains~~ has many glaciers, is higher than the eastern and western ~~flanks~~ parts. Post-glacier retreat GMCs consisting of ~~dead~~ buried ice and debris are widely distributed at glacier fronts (Shatravin, 2007). These GMCs are distinct from debris-covered glaciers, ~~and the~~ lakes forming on ~~them~~

GMCs are typically small, thermokarst-type, and non-stationary, and thermokarst type, although some are connected by internal drainage channels, leading to GLOFs (Narama et al., 2018). Some GMC termini have evolved into glacier-derived rock glaciers. Climate change over recent decades has driven glacier and GMC shrinkage and degradation of both glaciers and GMCs (Erokhin et al., 2017; Daiyrov et al., 2022).

On the northern flank of the central part of the Kyrgyz Range, total, 483 glaciers covering approximately 520 km² between 3,100 and 4,200 m elevation have been identified (Usabaliev et al., 2013), mainly concentrated mostly in the central river basins including Issyk-Ata, Alamudun, West-Karakol, and Sokuluk river basins (Maksimov and Osmonov, 1995; Usabaliev et al., 2013). In the Ala-Archa basin, glacier area decreased by 15.2–18% between 1963/64 and 2003–2010 (Aizen et al., 2006; Bolch, 2015). The Golubin Glacier (5.42 km²) is the largest in the Kyrgyz Range, and has with a long-term mass balance of averaging -0.20 ± 0.42 m w.e. yr⁻¹/year from 1949/50 to 2020/21 (Azisov et al., 2022). The largest GMC (~3 km²) is located at the Ken-Tor glacier front in the Noruz River basin (Figs. 1 and 6, Maksimov and Osmonov, 1995). Precipitation peaks between March and July, with an average annual precipitation of 787 mm and a mean annual temperature of -3.5°C (1969-2005) at the Teo-Ashuu meteorological station (3,400 m) in the central part of the range. Precipitation is a critical factor controlling influencing glacier mass balance in this region (Ponomarenko, 1976; Aizen et al., 2006).



80 **Figure 1: Maps of the study area in the Kyrgyz Range, northern Tien Shan. The top map shows the Kyrgyz Range, with glacial lakes in 2021 marked by red circles. The bottom left map highlights study sites in Kyrgyzstan. The Kyrgyz Range is divided into three sections by white dotted lines. Glacial lake sizes correspond to circle diameters.**

3 Methods

3.1 Satellite data collection

85 To quantify ~~the~~ historical changes in glacial lakes and glaciers ~~within~~ the Kyrgyz Range, we ~~used~~ utilized a combination of satellite remote sensing datasets spanning five decades using Corona, Landsat 7/ETM+ and Sentinel-2. Thirteen ~~near-near-~~ cloud-free Corona KH-4 stereo photographs from 1964 and 1968 ~~formed-provide~~ provide the earliest dataset, covering 2% (~~predominantly-mainly~~ 14 glaciers on the eastern part) and 98% of the study region, respectively. Each image ~~spans-covers~~ covers ~~about-~~ 16 km in width, with a spatial resolution between 1.8 and 2.7 ~~meters~~ meters (Table 1). DEMs and orthoimages were generated
90 from forward and aft stereo ~~-image~~ image pairs using Metashape (Agisoft), ~~and-with~~ and geometric distortions ~~were~~ corrected ~~using-via~~ via a non-metric camera model. Ground control points (GCPs) for geometric correction were systematically ~~selected-chosen~~ chosen from stable terrain features, such as large boulders, outside glacier and GMC areas. Coordinates were ~~taken-derived~~ derived from ~~QuickBird images in~~ Google Earth's ~~QuickBird images-~~ QuickBird images and advanced land observing satellite/panchromatic remote sensing instrument for stereo mapping (ALOS/PRISM) ortho-images (2.5 m resolution) ~~acquired in-dated~~ dated 2007, while vertical references ~~were~~
95 ~~based-originated on the from-high mountain Asia (HMA) DEM-data~~ (8 m resolution) from 2017. Each ~~each-~~ stereo pair, ~~processing-employed~~ 25–30 GCPs ~~were used and grouped into segmented-into~~ four ~~sub-areas-groups~~ sub-areas (a–d), ~~and carefully excluding~~ and carefully excluding cloudy or snow-covered features ~~were excluded-to to ensure-preserve~~ to ensure accuracy. The final Corona-derived DEM and orthophotos ~~have spatial resolutions of-achieved~~ achieved 4.1 m and 2.0 m ~~-spatial-resolutions~~ spatial resolutions, respectively. We also used orthoimages ~~from-of~~ Landsat 7/ETM+ ~~acquired~~ in 2000 (15 m) and Sentinel-2 (~~10-m~~) in 2021 (~~10 m~~; Table 2). ~~We used-~~ Landsat 7 pan-
100 sharpened images ~~were generated-converted~~ converted from 15 m panchromatic (~~8-band-8~~) and 30 m multispectral ~~bands-images~~ bands using ArcGIS Pro. ~~Only-These~~ Only scenes without ~~minimal-significant~~ minimal cloud or snow ~~coverage-contamination~~ contamination were ~~selected-used from~~ selected for ~~analysis-~~ analysis to maintain data quality and reliability.

Table 1: List of Corona KH-4 images of the study area.

Satellite	Corona Scenes	Date	Ground resolution (m)	Coverage area in study area (%)
KH-4A 10 (Corona 85, Mission 1010, OPS 3497)	DS1010-2086DA121	20.09.1964	2.7	east part : 2%
	DS1010-2086DA120			
	DS1010-2086DF114			
	DS1010-2086DF115			
KH-4A 48 (Corona 128, Mission 1048, OPS 0165)	DS1048-1039DA030	18.09.1968	2.7-7.6	west, central and east part: 74%
	DS1048-1039DA031			
	DS1048-1039DA032			
	DS1048-1039DF030			
	DS1048-1039DF031			
KH-4B 4 (Corona 127, Mission 1104, OPS 5955)	DS1104-2185DF053	07.08.1968	1.8	central-south and east part: 24%
	DS1104-2185DA057			
	DS1104-2185DA058			

105

3.2 Mapping of glacial lakes, glaciers, and GMCs

To ~~assess~~ understand the changes in the ~~of the~~ areas and numbers of glacial lakes in the Kyrgyz Range since 1960s, we manually digitized ~~glacial~~ lakes from Corona KH-4 images (1964, 1968), Landsat 7/ETM+ (2000), and Sentinel-2 (2021) using ArcGIS Pro (Table 2). Manual mapping ~~provides~~ ensures higher delineation accuracy ~~than compared to~~ semi-automated methods, ~~although~~ boundary uncertainties ~~remain~~ persist at pixel-scale level interfaces between water and land. Unclear ~~outline of lakes~~ outlines due to shadow in the Corona imagery were ~~evaluated~~ assessed using slope data from the Corona DEM; ~~areas~~ regions with ~~slopes less than~~ $\leq 10^\circ$ slope in uncertain zones were ~~cautiously~~ included as lake area ~~only when~~ if visually plausible, otherwise ~~they were~~ excluded to ~~avoid~~ prevent overestimation. Snow-covered and cloud-covered areas did not affect lake mapping; ~~because as they did not were~~ coincide with ~~areas without glacial lakes~~ locations.

We ~~applied~~ implemented a series of pre-processing steps in ArcGIS Pro to ensure ~~both~~ spatial and spectral consistency between Landsat 7 and Sentinel-2 images. For stable land areas, we ~~confirmed~~ verified that pixel values from ~~both the two~~ sensors were comparable and that normalized difference vegetation index (NDVI) values indicated similar vegetation cover, ~~thereby ensuring~~. ~~These checks confirmed~~ that the datasets ~~were suitable for temporal comparison~~ could be reliably compared for subsequent analysis. For image composition, ~~we selected~~ Landsat 7 bands 1, 2, and 3 ~~were used~~ to create an RGB composite ~~suitable~~ for water ~~detection~~ feature delineation, and ~~mapped~~ lake outlines ~~were mapped~~ from Sentinel-2 imagery (10 m resolution) using the corresponding ~~visible~~ bands ~~1, 2, and 3~~. To maintain consistency in ~~glacial~~ lake detection across the multitemporal imagery, we ~~adopted~~ set a minimum mapping threshold of 0.00045 km², equivalent to two pixels of 15-m Landsat image, ~~and~~. ~~This threshold was uniformly~~ applied ~~this uniformly~~ to Corona, Landsat 7, and Sentinel-2 datasets; ~~thus~~

125

~~permitting temporal comparisons of lake area change.~~ After manual delineation of lake boundaries, we calculated lake ~~parameters areas~~ and classified ~~each lakethem~~ as either contactless or glacier-contact-~~types~~. Area changes for individual lakes were quantified for ~~the years~~-1968, 2000, and 2021, and ~~temporal~~ shifts in lake type composition ~~over time~~ were also assessed.

130 Although manual mapping of lake polygons yields higher accuracy than semi-automated techniques, it ~~remains~~
~~sensitive is subject~~ to image-~~quality~~ ~~limitations issues~~ such as ~~boundary~~ ~~ambiguosity margins~~ at lake ~~edges margins~~ (Hanshaw
and Bookhagen, 2014). This ~~ambiguity~~ arises because pure-~~water~~ pixels often ~~bordered join~~ mixed pixels containing both
water and land, making ~~edge precise~~ classification ~~difficult of edge pixels challenging~~. To ~~estimate account for area these~~
uncertainty~~ties~~, we followed ~~the method of~~ Hanshaw and Bookhagen (2014) ~~and to~~ ~~excluded lakes with highly estimate area~~
~~error, and excluded lakes with~~ ambiguous boundaries from ~~further our~~ analysis. To ~~evaluate further assess~~ sensor-related
135 uncertainty, we selected a stable reference lake outside the GMC zone ~~that was~~, clearly visible in all image types. ~~Manual~~
~~delineation u~~Using consistent NDWI-~~based~~ thresholds, ~~we manually delineated this lake for each sensor and compared the~~
~~mapped area enabled direct comparison of mapped lake areas across sensors. The analysis showed that~~ Landsat 7 ~~yielded~~
~~produced~~ slightly larger lake areas ~~estimates~~ than the 1968 ~~Corona~~ reference (absolute difference: 0.000326 km²; relative
140 km²; relative difference: 8.8%), whereas Sentinel-2 (2021) provided results closer to the ~~reference baseline~~ (absolute difference: 0.000127
km²; relative difference: 3.4%). The ~~finer superior~~ spatial resolution of Sentinel-2 contributed to ~~a~~ more precise delineation.
~~An uncertainty of about~~ ~~Nevertheless, an~~ 8.8% ~~was considered uncertainty margin is generally~~ acceptable for ~~manual~~ glacial
lake mapping ~~when using Landsat data, and~~ ~~and manual mapping. Consequently, we adopted~~ this reference lake ~~was used to~~
~~represent for estimating~~ overall sensor-related ~~error uncertainty~~. The consistency of these ~~estimates with findings with our~~
145 previous work in the Kyrgyz Range ~~supports the robustness of our approach~~ (Daiyrov et al., 2022) ~~further validates the~~
~~approach~~.

Glaciers were ~~also~~ manually mapped using Corona KH-4 imagery from 1964 and 1968, ~~as well as and~~ Sentinel-2 imagery from
2021. Only ~~scenes with images acquired under~~ minimal cloud and snow cover were ~~used selected for analysis~~ to ensure ~~reliable~~
~~accurate~~ boundary identification. All Corona images from 1968 and Sentinel-2 scenes from 2021 were ~~acquired in eaptured~~
~~during the~~ summer ~~months~~ (August for Sentinel-2, August-~~and~~ September for Corona), ~~thereby~~ minimizing ~~the influence of~~
150 seasonal snow-~~effects~~ (Table 1). Glacier ~~outlines boundaries~~ were delineated by visual interpretation of standard false-
~~color colour~~ composites ~~constructed~~ from multi-spectral imagery, ~~and~~ ~~G~~ glacier area changes between 1964/1968 and 2021
were ~~then quantitatively~~ calculated ~~from based on~~ these polygonal ~~outlines datasets~~.

Table 2: List of Satellite images for glacial lake extraction.

Satellite	Sensor	Date	Ground resolution (m)	ID:		
Landsat 7	Enhanced Thematic Mapper (ETM)	07.07.2000	30	LE07_L1TP_151031_20000707_20200918_02_T1		
		07.07.2000	30	LE07_L1TP_151030_20000707_20200918_02_T1		
		16.07.2000	30	LE07_L1TP_150030_20000716_20200918_02_T1		
		16.07.2000	30	LE07_L1TP_150031_20000716_20200918_02_T1		
		30.07.2000	30	LE07_L1TP_152031_20000730_20200917_02_T1		
		30.07.2000	30	LE07_L1TP_152030_20000730_20200918_02_T1		
		24.08.2000	30	LE07_L1TP_151031_20000824_20200918_02_T1		
		24.08.2000	30	LE07_L1TP_151030_20000824_20200917_02_T1		
		02.09.2000	30	LE07_L1TP_150031_20000902_20200917_02_T1		
		02.09.2000	30	LE07_L1TP_150030_20000902_20200918_02_T1		
		Sentinel-2 Multi-Spectral Instrument (MSI)		24.07.2021	10	S2A_MSIL2A_20210724T054641_N0500_R048_T43TEH_20230220T005731.SAFE
				11.08.2021	10	S2B_MSIL2A_20210811T055639_N0500_R091_T43TCH_20230215T033526.SAFE
11.08.2021	10			S2B_MSIL2A_20210811T055639_N0500_R091_T43TCG_20230215T033526.SAFE		
11.08.2021	10			S2B_MSIL2A_20210811T055639_N0500_R091_T43TDH_20230215T033526.SAFE		
11.08.2021	10			S2B_MSIL2A_20210811T055639_N0500_R091_T43TDG_20230215T033526.SAFE		
11.08.2021	10			S2B_MSIL2A_20210811T055639_N0500_R091_T43TEH_20230215T033526.SAFE		
21.08.2021	10			S2B_MSIL2A_20210821T055639_N0500_R091_T43TCH_20230210T193704.SAFE		
21.08.2021	10			S2B_MSIL2A_20210821T055639_N0500_R091_T43TCG_20230210T193704.SAFE		
21.08.2021	10			S2B_MSIL2A_20210821T055639_N0500_R091_T43TDH_20230210T193704.SAFE		
21.08.2021	10			S2B_MSIL2A_20210821T055639_N0500_R091_T43TDG_20230210T193704.SAFE		
21.08.2021	10			S2B_MSIL2A_20210821T055639_N0500_R091_T43TEH_20230210T193704.SAFE		
05.09.2021	10			S2A_MSIL2A_20210905T055641_N0500_R091_T43TCG_20230118T130151.SAFE		
05.09.2021	10			S2A_MSIL2A_20210905T055641_N0500_R091_T43TEH_20230118T130151.SAFE		
07.09.2021	10			S2B_MSIL2A_20210907T054639_N0500_R048_T43TEH_20230118T203059.SAFE		
27.09.2021	10			S2B_MSIL2A_20210927T054639_N0500_R048_T43TEH_20230124T140016.SAFE		

155

To map GMCs in the study area ~~were mapped based on~~, ~~we employed~~ several geomorphological criteria. GMCs were identified as continuous, debris-covered surfaces, up to 3 km ~~long in length~~ extending from the glacier fronts, lacking ~~distinct prominent~~ moraine ridges, and ~~showing exhibiting~~ a convex cross-sectional profile. The absence ~~of~~ ~~contiguous~~ ~~of surface valley bottom~~ drainage channels ~~at glacier fronts~~ was ~~checked through interpretation of~~ Google Earth imagery. ~~We also assessed~~ ~~the~~ presence of preserved ice within GMCs ~~was further assessed~~ using differential interferometric SAR (DInSAR) ~~analysis~~ to detect surface deformation. These GMCs ~~formed developed~~ during glacier retreat ~~after since~~ the Little Ice Age and typically ~~consist of comprise various moraine landforms and buried~~ ~~buried~~ ice and debris (Shatravin, 2007; Erokhin, 2011). GMCs ~~boundaries~~ were delineated according to these geomorphological characteristics and ~~existing boundaries established in previous~~ regional ~~mapping studies~~ (Maksimov, 1982; Maksimov and Osmonov, 1995; Shatravin and Stavisski, 1984; Shatravin, 2007; Erokhin, 2008, 2011). GMC ~~boundaries~~ were manually digitized ~~primarily from using~~ Sentinel-2 imagery ~~acquired from~~ in 2021, and ~~where image clarity was insufficient~~, higher-resolution Corona KH-4 images from 1964 and 1968 were ~~used where Sentinel-2 image quality was insufficient~~ ~~referenced to refine the delineations~~. All area ~~delineations were carried out mapping using~~ ~~fused~~ ~~false~~ ~~color~~ ~~colour~~ multi-spectral ~~composites imagery~~ acquired under conditions ~~of with~~ minimal cloud and snow cover.

160

165

170

3.3 Geomorphological analysis using DInSAR

To quantify ~~the number of~~ GMCs containing buried ice, we conducted DInSAR analysis using GAMMA SAR software and ALOS/Phase Array type L-band Synthetic Aperture Radar (PALSAR) and ALOS-2/PALSAR-2 (L-band) datasets. GMCs ~~exhibiting showing~~ surface displacement, ~~expressed~~ ~~— identified~~ as coherent ~~interference displacement~~ fringes representing ~~both~~ horizontal and vertical ground ~~movements~~, ~~—~~ were interpreted as likely containing significant ice content. ~~These~~ ~~D~~ displacement fringes ~~, revealed in the DInSAR results,~~ indicate active surface processes such as permafrost creep or ~~the~~ subsidence resulting from ~~the~~ melting of buried ice. ~~In addition, landform features such as thermokarst depressions, curved ice cliffs, and surface channels were considered in the mapping of GMCs.~~ The ~~processing technical approach~~ and interpretation followed established ~~methodologies from detailed in~~ previous ~~studies works~~ (Goldstein et al., 1997; Werner et al., 2001; Quincey et al., 2007; Sandwell et al., 2008; Daiyrov et al., 2018).

~~Our analysis employed b~~oth long-interval (>10 months, spanning winter) and short-interval (1–3 months, summer) ~~interferometric image~~ pairs ~~were used,~~ comprising 49 images ~~in total~~ (18 from ALOS/PALSAR ~~images from,~~ 2009–2010 ~~and;~~ 31 ~~from~~ ALOS-2/PALSAR-2 ~~images from,~~ 2014–2016), all with perpendicular baselines ~~<less than~~ 1,500 m (Table 3). ~~Table 3 provides a part of list of image pairs used.~~ The DInSAR ~~processing~~ workflow ~~included consisted of~~ converting raw SAR data to Single Look Complex (SLC) format, ~~coregistration of image pairs SLCs,~~ ~~generation of~~ differential interferograms, ~~removal of~~ topographic phase using Shuttle Radar Topography Mission (SRTM) DEM, ~~phase~~ unwrapping ~~interferometric phase~~ to obtain displacement ~~information,~~ and geocoding ~~results into~~ a geographic coordinate system. Noise from temporal and spatial decorrelation was ~~reduced suppressed~~ using an adaptive filter (Goldstein et al., 1997; Goldstein and Werner, 1998). In our results, ~~displacement fringes in~~ long-interval ~~interferograms mainly captured pairs primarily record~~ slow subsidence, ~~whereas those in~~ short-interval ~~interferogram pairs highlighted reveal~~ more rapid surface motion, ~~consistent with.~~ ~~This distinction follows~~ earlier ~~observations from findings, such as those for the Swiss Alps' Gruben rock glacier such as the Gruben rock glacier in the Swiss Alps,~~ where only short-interval interferograms ~~clearly successfully~~ detected surface motion (Strozzi et al., 2004).

~~DInSAR in high mountains is subject to limitations such as low scatterer density, atmospheric disturbances, and line-of-sight constraints, which can obscure displacement signals (Schlögl et al., 2022). Although L-band data have advantages over shorter wavelengths, issues such as low coherence, shadow, and foreshortening still affect the results in steep terrain (Atwood et al., 2010; Chen et al., 2025).~~ To ~~validate verify~~ the interpretation of buried ice within GMCs ~~based on DInSAR,~~ we compared ~~DInSAR-derived~~ surface motion ~~signals~~ at the Chelektor Glacier front with ~~locations of~~ known ~~internal~~ ice ~~occurrences,~~ and found ~~a good spatial correspondence that internal ice consistently corresponded with DInSAR detected displacement.~~ Additional ~~validation ground truthing~~ was ~~provided by performed using~~ GNSS measurements at the Adygine Glacier GMC, ~~which further supported the interpretation.~~ The presence of ~~active, ice-related deformation.~~ ~~Independent evidence from DInSAR and field survey in GMCs has also been confirmed in the Teskey Range has also confirmed ice-rich GMCs in~~ the northern Tien Shan ~~by both DInSAR and field surveys~~ (Daiyrov et al., 2018). Areas ~~showing of~~ pronounced deformation were

also analyzed using DEM differencing (HMA, 2017 and UAV, 2018), which indicated substantial surface changes ~~coincident~~ with mapped buried ice ~~zones~~. ~~Consequently~~ Thus, ~~DInSAR detected~~ deformation ~~detected by DInSAR~~ in GMCs ~~moraine complexes~~ is interpreted as evidence of ice-rich conditions, with melt-induced subsidence as the ~~most plausible~~ ~~probable~~ mechanism (Daiyrov et al., 2018).

Table 3: List of ALOS data (a part of data).

Pair	Master ID	Slave ID	Master Date (YYYYMMDD)	Slave Date (YYYYMMDD)	Span (days)	Bperp (m)	Orbit	Offnadir angle(°)
A	ALOS2015180840-140903	ALOS2058650840-150624	20140903	20150624	294	100.4	Ascending	36.2
B	ALPSRP239030840	ALPSRP245740840	20100720	20100904	46	337	Ascending	34.3
C	ALPSRP079740840	ALPSRP240780840	20070724	20100801	1104	1332.7	Ascending	34.3
D	ALOS2064120840-150731	ALOS2074470840-151009	20150731	20151009	70	90.9	Ascending	32.5
E	ALOS2018580840-140926	ALOS2072400840-150925	20140926	20150925	364	-14.2	Ascending	28.2
F	ALPSRP236550840	ALPSRP243260840	20100703	20100818	46	143.3	Ascending	34.3

3.4 Geomorphological analysis using DEMs and their accuracy assessment

Widespread formation of surface depression (thermokarst feature) on glaciers and GMCs is attributed to surface subsidence caused by melting buried ice (Erokhin et al., 2017; Narama et al., 2010, 2018; Daiyrov et al., 2018; Daiyrov and Narama, 2021). To investigate long-term morphological changes of GMCs, we compared DEMs derived from Corona ~~in (1968)~~ and HMA DEMs (2017). In addition, ~~to investigate morphological changes of GMC, field surveys using~~ unmanned aerial vehicles (UAVs) ~~surveys~~ were conducted for GMC ~~at the~~ Chelektor Glacier ~~in the~~ central ~~part of the~~ Kyrgyz Range in ~~the~~ summers of 2018 (15 July) and 2023 (28 July), generating complementary high-resolution data. The 2018 ~~survey campaign~~ mapped the entire GMC, whereas 2023 ~~survey focused mainly on the glacier terminus because of coverage was partial due to unfavorable/unfavourable weather, focusing primarily on the glacier terminus. UAV data acquired by a~~ The Phantom4 RTK platform (DJI) ~~were captured geotagged imagery~~ processed in Pix4Dmapper to ~~generate yield~~ orthoimages ~~with a spatial resolution of~~ 5.4 m and DEMs ~~with a resolution of at~~ 1.0 m ~~resolution~~.

~~Vertical changes were quantified by~~ Finally, ~~the amount of vertical decline was calculated by~~ comparing ~~multiple DEMs~~: Corona (4.1 m resolution, 1968), SRTM (30 m, 2000), HMA (8 m, 2017), and UAV DEMs (1.0 m, 2018 and 2023). Surface depression polygons for 1968, 2000, 2017, 2018, and 2023 were generated using a hydrologic ‘filling’ algorithm in ArcGIS Pro to ~~allow~~ ~~quantitatively~~ ~~assessment of depression~~ area changes over time. The vertical accuracy of these datasets was evaluated ~~relative to the~~ ~~against~~ HMA DEM, which ~~was used as a stable~~ ~~provides an accurate, temporally consistent terrain~~ reference. ~~Stable, nonglacier terrain outside areas devoid of glacier and GMCs was~~ ~~ere~~ selected as benchmark ~~areas, and s-~~ ~~Elevations~~ ~~data~~ from ~~the~~ Corona, SRTM, and UAV DEMs were ~~vertically~~ aligned to ~~match~~ HMA reference elevations, ~~to~~ ~~correcting~~ systematic ~~vertical~~ offsets. ~~Subsequently, e~~ Elevation differences ~~between each corrected DEM and the HMA DEM of the corrected DEMs~~ were ~~then calculated~~ ~~computed~~ within polygon area around ~~the~~ stable ~~reference~~ points. ~~The~~ Root Mean Square Error (RMSE) values were ~~within acceptable ranges for geomorphological analysis:~~ 2.2 m for Corona DEM, 2.8 m for SRTM ~~DEM~~, and 1.3 m for UAV ~~DEM, which are acceptable for geomorphological analysis at the study scale and given the~~

local relief. However, the relatively sparse GCPs for Corona and the coarse resolution of SRTM limit the ultimate vertical precision of these datasets. These error margins are appropriate considering the study scale and the terrain's elevation gradients, although Corona's limited GCP density and SRTM's coarse resolution limit their ultimate vertical fidelity.

4 Results

4.1 Changes in glacial lake numbers and areas during 1968–2021

We identified 274 glacial lakes in 1968, 380 lakes in 2000, and 412 lakes by 2021 (Fig. 2), demonstrating that the total number of glacial lakes in the Kyrgyz Range effectively nearly doubled over the study period. Of the original 274 lakes present in 1968, 190 (69%) had disappeared by 2000, and similarly, of the 380 lakes mapped/observed in 2000, 142 had disappeared by 2021. In contrast, 84 lakes have persisted from 1968 through 2021. Substantial renewal occurred, with 154 new lakes (41% of the total in 2000) appeared between 1968 and 2000, and a further 175 new lakes (42% of the total in 2021) formed between 2000 and 2021 observed in each subsequent time step. Notably, one lake that had vanished by 2000 reappeared by 2021 (Fig. 2). The high rates of both lake disappearance and new formation indicates a highly dynamic regime/process of glacial lake renewal, in which contrasts to the more gradual and continual expansion of glacial lakes observed/reported for the eastern Himalayas since the mid-twentieth century (Yamada, 1998; Ageta et al., 2000; Iwata et al., 2002; Komori et al., 2004). This study used >0.1 km² threshold and they got 773 lakes. By contrast, there is no lakes of >0.1 km² in our study area. This pattern of rapid lake formation and loss is consistent with trends reported for the Kungoy and Ili Ranges, also within the northern Tien Shan (Narama et al., 2009).

Figure 3 illustrates/shows the distribution of lakes by size class over time. In 1968, small lakes (0.00045–0.001 km²) comprised/accounted for 36% of all glacial lakes, but while by 2000 and 2021, this proportion declined/had decreased to 18–22% in 200 and 2021. Medium-sized lakes (0.001–0.01 km²) dominated total lake area/the area spectrum, contributing/accounting for 60% of the total lake area in 1968, rising to 78% in 2000, and 71% in 2021. The number of large lakes (0.01–0.1 km²) increased from 11 in 1968 to 30 in 2021, and the total area of these lakes expanded 2.6-fold, from 0.23 km² to 0.59 km². A total of 773 glacial lakes larger than 0.1 km² have been identified in the Bhutan Himalayas (Nagai et al., 2017), whereas no glacial lakes exceeding 0.1 km² are present in the Kyrgyz Range.

The cumulative glacial-lake area increased from 0.80 km² in 1968 to 1.20 km² in 2000, and then by a further 18% to 1.42 km² by 2021 by 2021, the area had increased by an additional 18% to reach 1.42 km². Among the 84 lakes that persisted for the entire study period, area changes were significant: 14 exhibited marked/substantial variability, with area changes ranging from 0.005 to 0.053 km² between 1968 and 2021. Of the lakes present in 2000, 152 experienced areal variation, including 13 with marked increases (0.005–0.053 km²) between 2000 and 2021. Spatial analysis further shows that the largest lakes predominantly formed at the termini of retreating glaciers, while most medium and small lakes developed on GMCs farther from present/active glacier termini/ice.

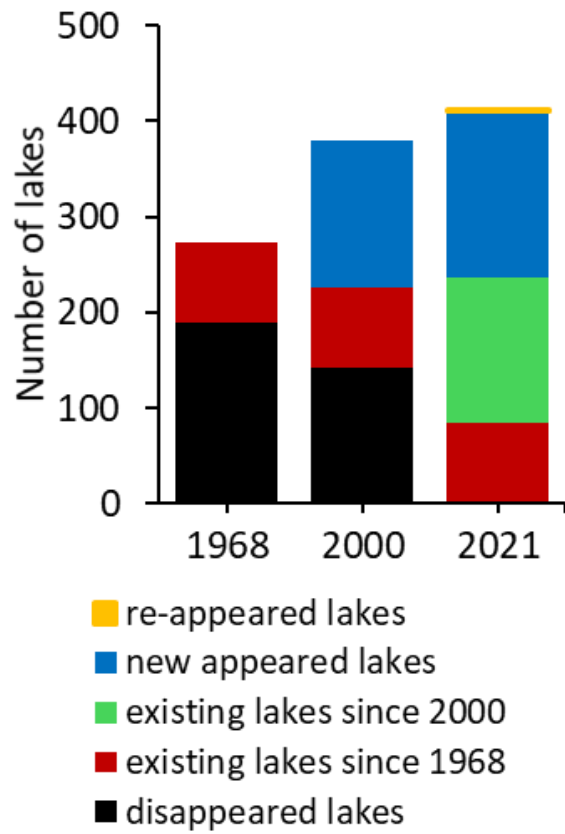


Figure- 2. Numbers of glacial lakes and their changes in 1968, 2000 and 2021.

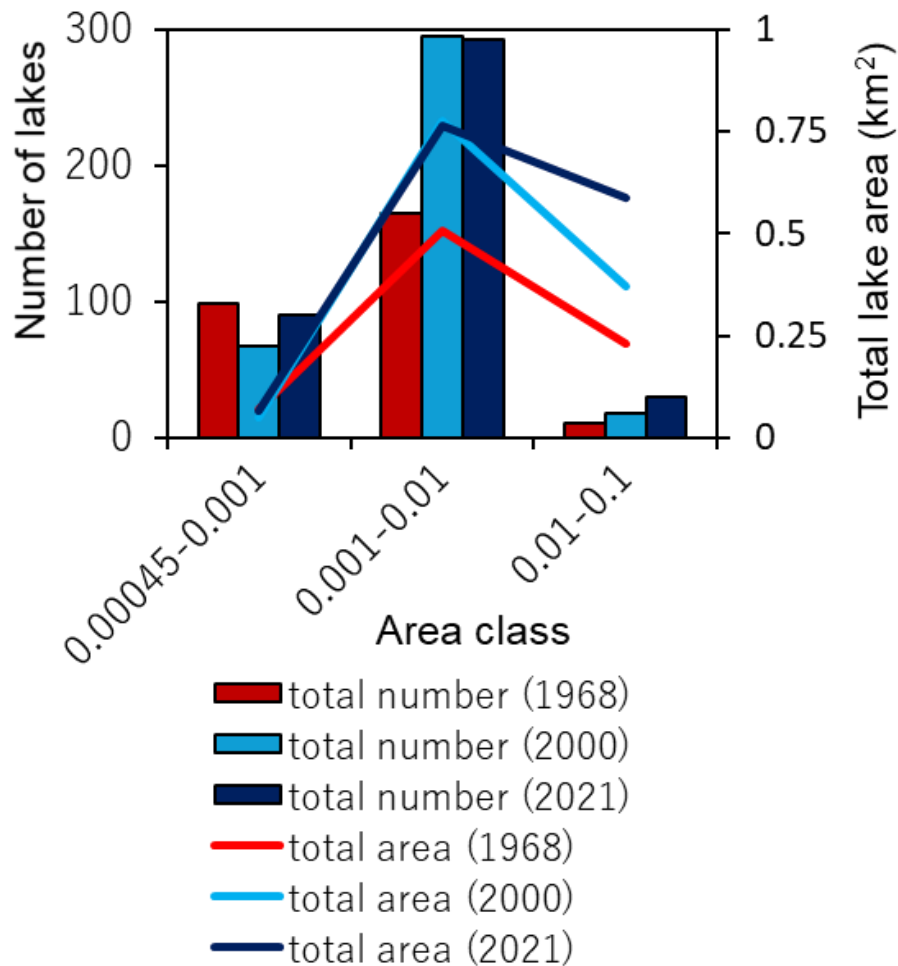


Figure 3: Numbers and areas of glacial lakes in the three area classes in 1968, 2000 and 2021.

4.2 Types of glacial lakes and their evolution

In this region, glacial lakes were classified into two ~~main principal~~ types based on their spatial relationship to glaciers: glacier-contact (proglacial) lakes and contactless (thermokarst) lakes (Fig. 4a). The classification was determined solely by the current location of each lake relative to the glacier margin, rather than differences in genesis. Glacier-contact lakes are situated adjacent to glacier termini and are typically impounded by GMCs, moraines, or bedrock. In contrast, contactless lakes—primarily thermokarst in origin—form on the surface of GMCs as a result of the melting of buried ~~glacier~~ ice. Some thermokarst lakes ~~exhibit show~~ pronounced seasonal variations in surface area, including phases of stability, expansion, ~~contractions~~ shrinkage, ~~appearance~~ emergence, disappearance, and short-lived existence (Daiyrov et al., 2018), similar to —phenomena often observed in—supraglacial lakes on debris-covered glaciers due to their connection with evolving drainage channels (Narama et al., 2017;

Sakurai et al., 2021)(Daiyrov et al., 2018). In addition, More detailed lake classifications of the lakes in for the study area can be found have been presented in previous reports (Erokhin, 2008, 2011; Janský et al., 2006, 2010).

280 Long-term analysis reveals a notable shift in lake types over time (Fig. 4b). While 45% (124 of the 274) of the lakes identified in 1968, 45% (124 lakes) were contactless, increasing this proportion rose to 72% (272 of 380) in 2000 and 71% (291 of 412) in 2021, indicating a significant increase in the number of thermokarst lakes on GMCs. Conversely, the number of glacier-contact lakes has steadily decreased since 1968. As illustrated in Fig 4c, the fate of individual lakes underscores these trends: of the 150 glacier-contact lakes present in 1968 (including one documented in 1964), only 26 remained classified as glacier-contact lakes by 2021, 36 had transitioned to contactless status due to glacier retreat, and 88 had disappeared altogether. Of the 124 contactless lakes identified in 1968, 55 persisted through 2021 while 70 ceased to exist disappeared.

285 These results highlight indicate that, unlike the eastern Himalayas—where glacier-contact lakes can persist and expand over extended periods (Yamada, 1998; Nagai et al., 2017)—glacier contact such lakes in the Kyrgyz Range tend to be transient. Here, Rapid glacier retreat combined with generally steep glacier-front slopes tends to separate former contact lakes from glacier termini, and while the limited development of large GMCs and flat outwash plains further constrains impedes the sustained expansion and longevity of glacier-contact lakes (Agarwalet al., 2023).

290

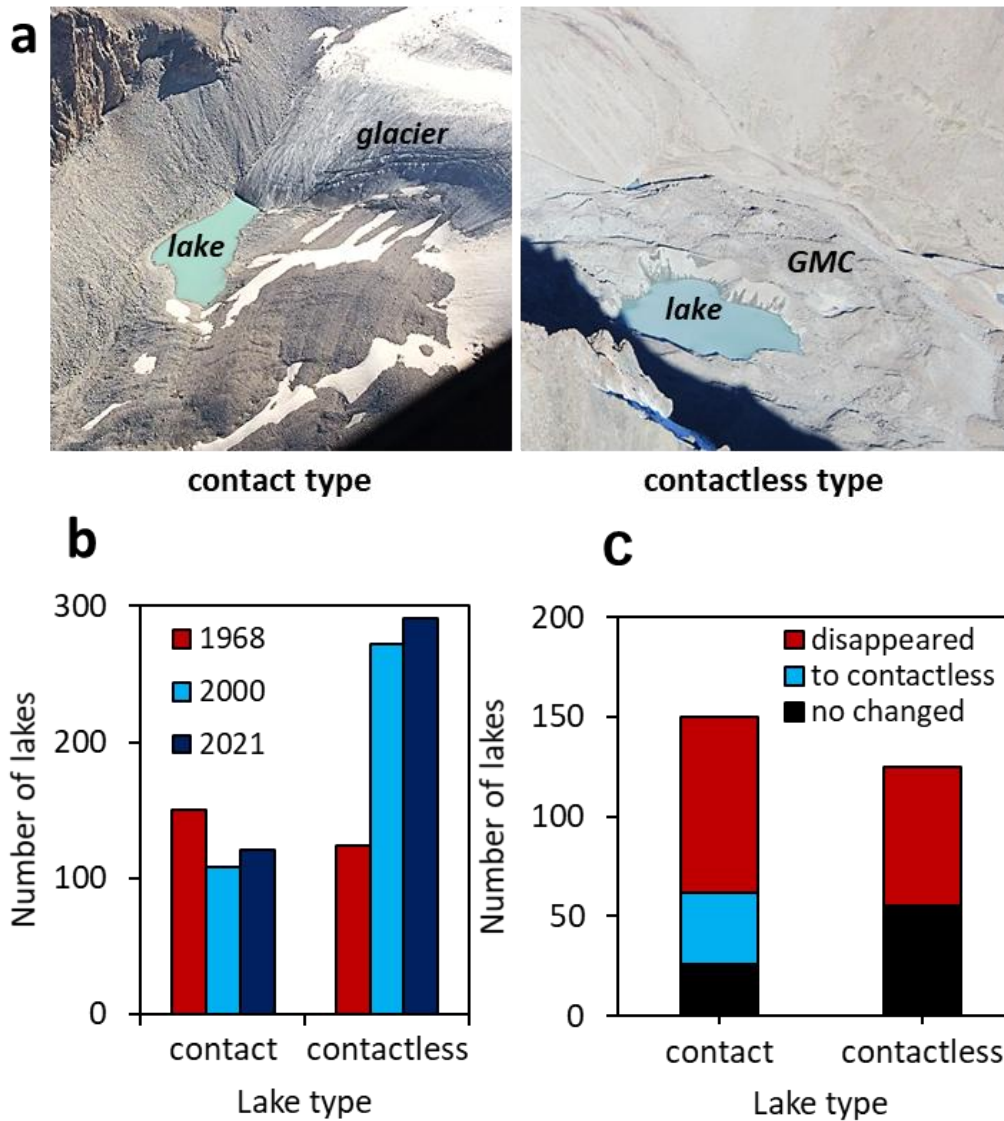


Figure 4: a) Photographs of the two types of glacial lakes: glacier-contact (left); contactless (right) . b) Comparison of the number of glacial lakes by type in 1968, 2000, and 2021. c) Transitions in lake type from 1968 to 2021.

295 4.3 Area changes in glaciers and surface changes in GMCs

To clarify and date the processes behind and underpinning the recent formation and disappearance of glacial lakes, we analyzed temporal changes in both glacier extent and glacier moraine complexes (GMCs) were analyzed across the Kyrgyz Range between for the period 1968 and 2021. Substantial retreat of glacier termini occurred across the range, converting throughout this period, resulting in the transformation of recently deglaciated terrain area into GMCs (Fig. 5a). The total glacier area

300 decreased from ~~390378.53~~ km² in 1968 to ~~2625.40~~ km² in 2021, reflecting a reduction of ~~3231~~% over 53 years (Fig. 5b). Spatially, ~~7270~~% of the glacierized area was concentrated in the central ~~part of the~~ Kyrgyz Range, while the western and eastern ~~sector/parts~~ accounted for 19% and ~~910~~%, respectively. The relative ~~rates of glacier shrinkage rates~~ were ~~3037~~% in the central ~~part/region~~, ~~3627~~% in the west, and 40% in the east. ~~Our analysis shows that~~ ~~The number of glaciers decreased from 787 in 1968 to 757 in 2021, despite fragmentation of~~. ~~Although~~ ~~Note that many~~ ~~some~~ large glaciers ~~have~~ ~~are~~ ~~fragmented~~ into smaller ones that glaciers, ~~increas~~ ~~ed~~ ~~ing~~ ~~their~~ ~~total~~ ~~glacier~~ ~~counts~~ ~~number~~ (Bolch et al., 2015). ~~the overall number of glaciers has nevertheless declined~~. This is because small glaciers disappeared after separating from larger parent glaciers. ~~Glacier fragmentation often produced~~ ~~leads to the formation of multiple GMCs within a single glacier basin, some of which may evolved into independent units as the source glaciers completely disappeared (Shatravin, 2007; Erokhin, 2011).~~ ~~This process can also favored the formation result in the development of numerous small lakes (Izagirre et al., 2025). However, not all glaciers in the Kyrgyz Range have formed GMCs.~~

We identified ~~611-521~~ GMCs in the Kyrgyz Range. Focusing on GMCs ~~that~~ ~~particularly those~~ host ~~to~~ numerous contactless (thermokarst) lakes. ~~our~~ comparison of DEMs from Corona (~~in~~ 1968) and HMA (~~in~~ 2017) showed that ~~44250~~ GMCs (~~4841~~%) of the ~~total 611-521 GMCs in the Kyrgyz Range~~ experienced substantial surface lowering of -5 to -30 meters. ~~Extensive-Large~~ vertical declines (-10 to -30 m) were especially ~~widespread~~ ~~evident~~ in GMCs ~~with~~ in the Sokuluk, Jylamysh, Ala-Archa, Alamudun, Noruz, Issyk-Ata, and Kegeti river basins (Fig. 1). DInSAR data ~~covering for~~ 2007–2010 and 2014–2016 further revealed that ~~450-396~~ (~~7465~~%) of ~~611-521~~ GMCs ~~underwent~~ ~~show~~ significant displacement, ~~a signal that is consistent with surface adjustment attributable to the deformation driven by melting of buried ice (Fig. 5c; Daiyrov et al., 2018; Daiyrov and Narama, 2021). These DInSAR results also enabled identification of GMCs with high/strong potential for future lake formation, as showing by displacement patterns on interferograms from summer 2009 and 2010 (Fig. 6). This significant surface changes occurred mainly on GMCs during summer and were closely related to subsidence from buried ice melt and creep of internal ice. The most pronounced deformation was observed in GMCs in the Sokuluk, Ala-Archa, and Issyk-Ata basins, whereas about 20% of GMCs showed no detectable deformation, implying ice-free or only weakly active conditions. Areas without displacement were likely ice-free or degraded area (Buchelt et al., 2024; Kunz et al., 2022, 2025), indicating not all GMCs still contain buried ice.~~

325 At the Chelektor Glacier GMC, ~~a~~ representative site in the central ~~part of the~~ range, ~~three~~ surface depressions (thermokarst feature) formed between 1968 and 2017 (Fig. ~~6a7a~~,b). Morphological evidence ~~from~~, ~~such as~~ imagery and DEM differences, clearly ~~shows~~ ~~demonstrate~~ that ice melt induced both surface subsidence and depression formation (Fig. ~~6e7c~~). From 2000 to 2021, depression-1 ~~grew~~ ~~expanded~~ substantially (Fig. ~~6d7d~~), and; ~~repeate~~ ~~comparative~~ photographs from 2015 and 2018 ~~capture~~ ~~highlight~~ these rapid ~~morphological~~ changes (Fig. ~~7a8a~~,b). Over a three-year interval, the surface area of the depression nearly doubled. Elevation profiles (Fig. ~~7e8c~~,f) ~~document~~ ~~reveal~~ a maximum surface lowering of -23 m for depression-1 and -28 m for depression-2, ~~indicating~~ ~~substantial~~ ~~confirming~~ ~~significant~~ geomorphic ~~modification~~ ~~evolution~~. As ~~the~~ Chelektor Glacier retreated, new glacial lakes formed within these depressions, ~~demonstrating the tight coupling~~ ~~illustrating the close linkage~~ between glacier ~~dynamics~~ ~~retreat~~, GMC transformation, and lake ~~development~~ ~~formation~~ (Fig. ~~7d8d~~,e).

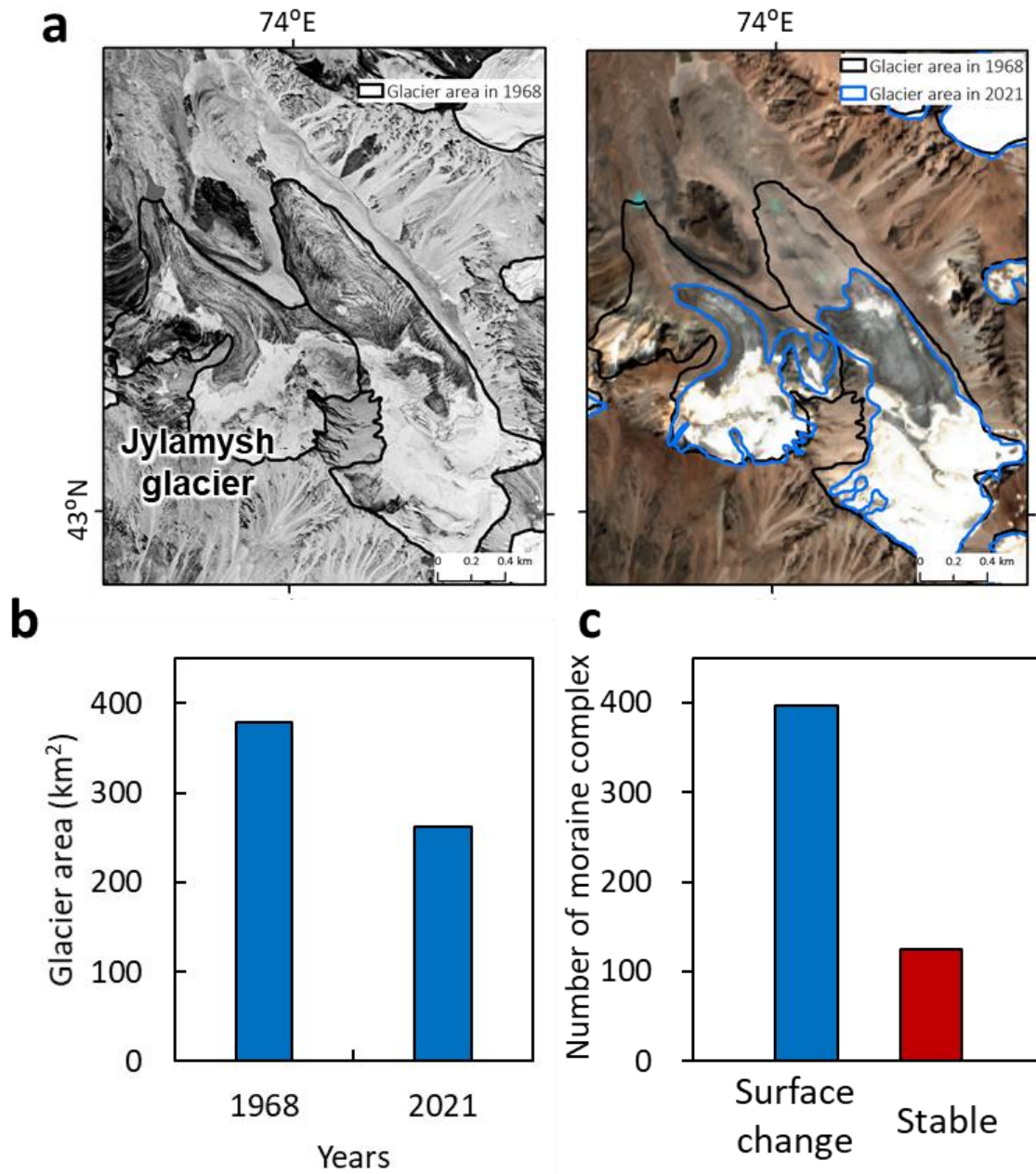


Figure 55: a) Glacier shrinkage in the Kyrgyz Range, illustrated by satellite images from different years: Corona KH-4B (1968, left) and PlanetScope (2021, right). b) Changes in glacier area in the Kyrgyz Range between 1968 and 2021. c) Number of GMCs detected at the surface changes based on DInSAR data.

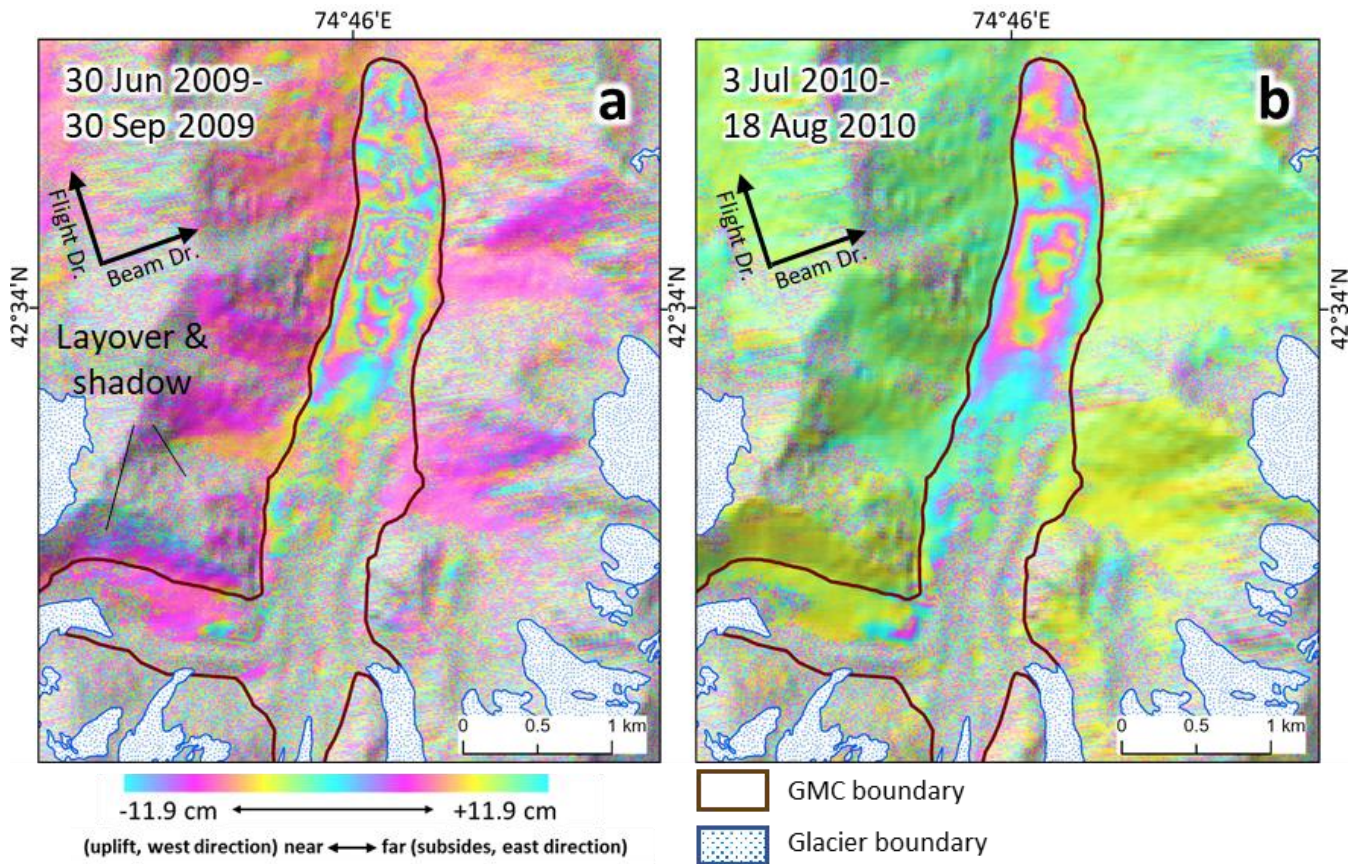
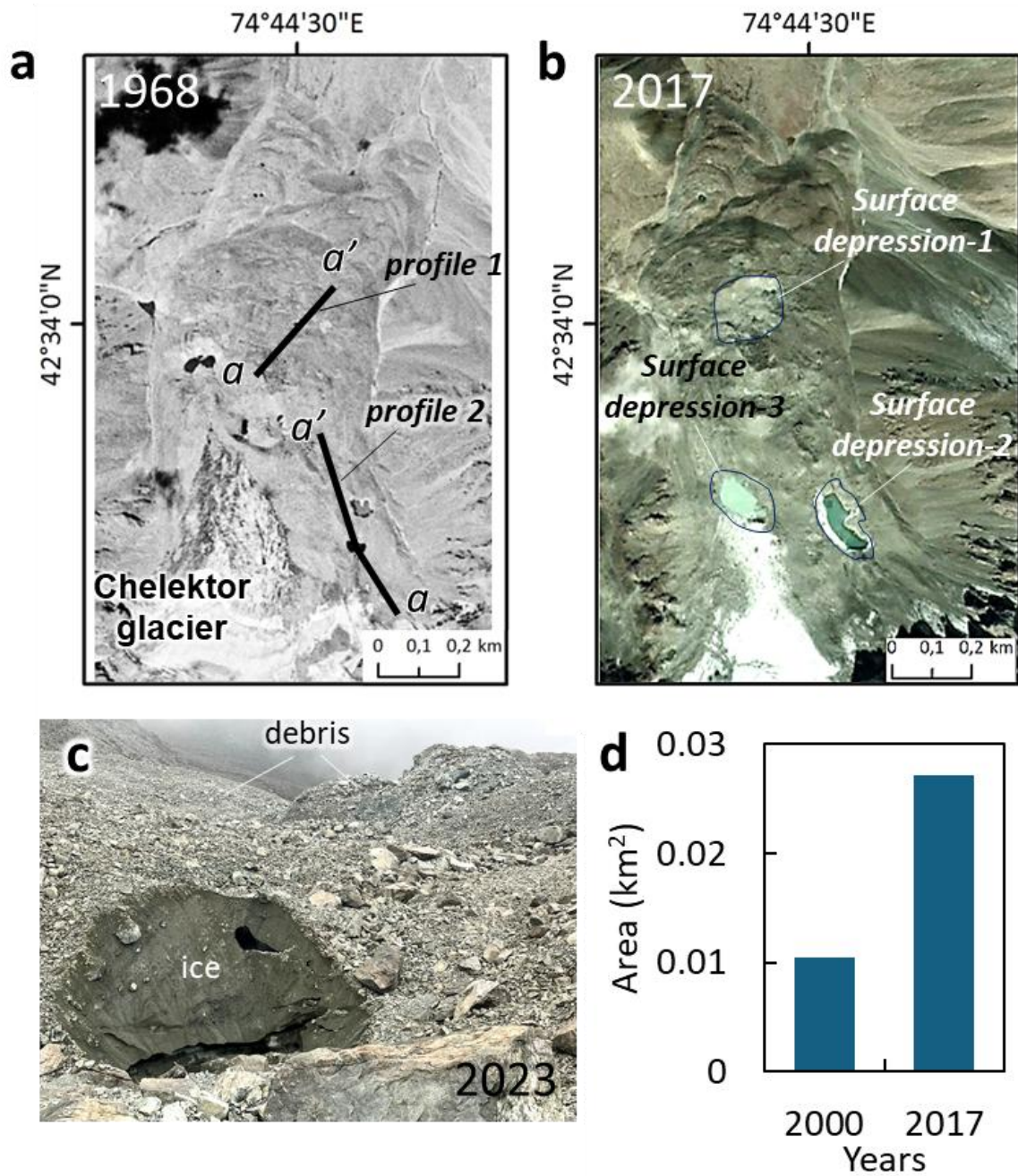


Figure 6. Aa, b): Seasonal surface change on GMC based on DInSAR analysis in summers of 2009 and 2010 using ALOS/PALSAR (Ken-Tor Noruz-GMC, location in Fig. 1). Displacement patterns correspond to subsidence and minor creep movements, interpreted as evidence of buried ice melt and surface instability.



350

Figure 67: a–b) Development of a surface depression on GMC at the Chelektor Glacier front (location in Fig. 1), illustrated by satellite images from different years: Corona KH-4B (1968, left) and PlanetScope (2017, right). c) Exposed ice on GMC. d) Area changes of surface depression-1 from 2000 to 2017.

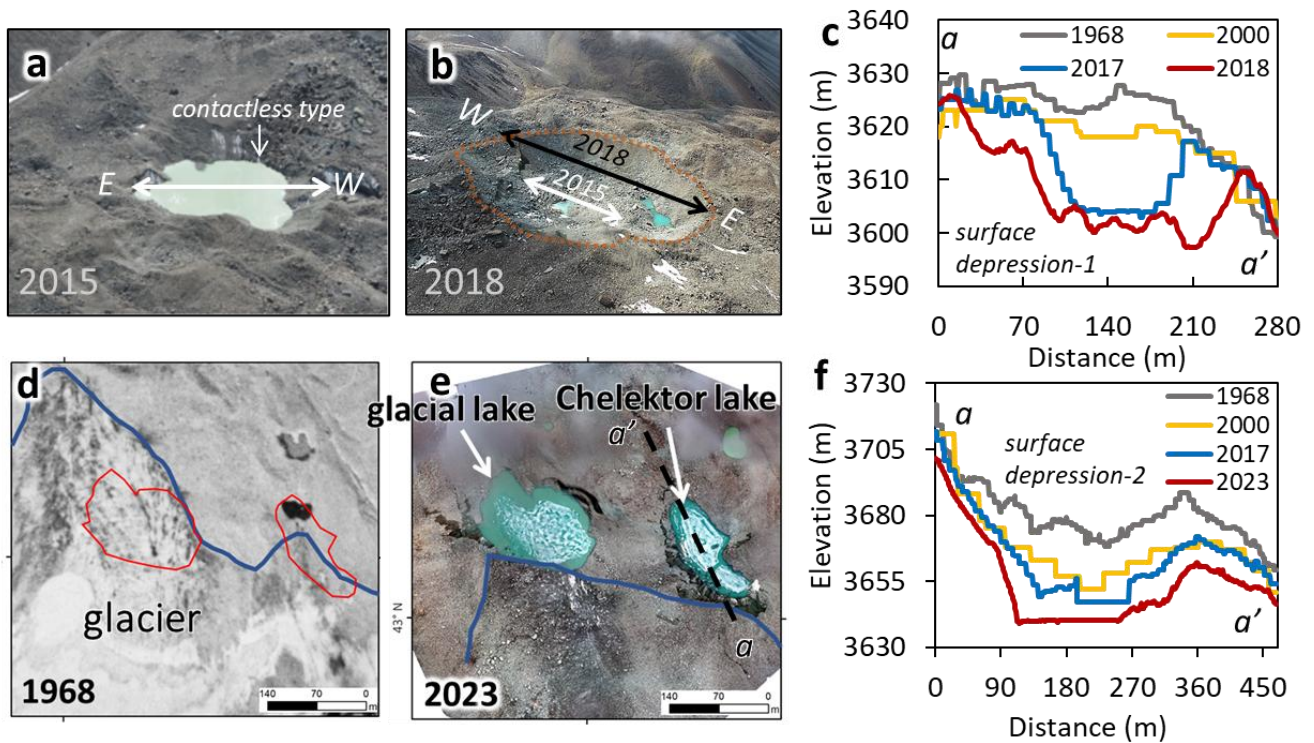


Figure 78: Surface depression development and the formation of new glacial lakes on GMC at the Chelektor glacier front. a, b) Photographs of surface depression-1 in 2015 and 2018. c, f) Changes in surface depression profiles (profile lines indicated in Fig. 6a). d) Orthoimage from Corona (1968). e) UAV orthoimage from 2023. Profile data are derived from DEMs of 1968 (Corona), 2000 (SRTM 1), 2017 (High Mountain Asia), and 2018-2023 (UAV data).

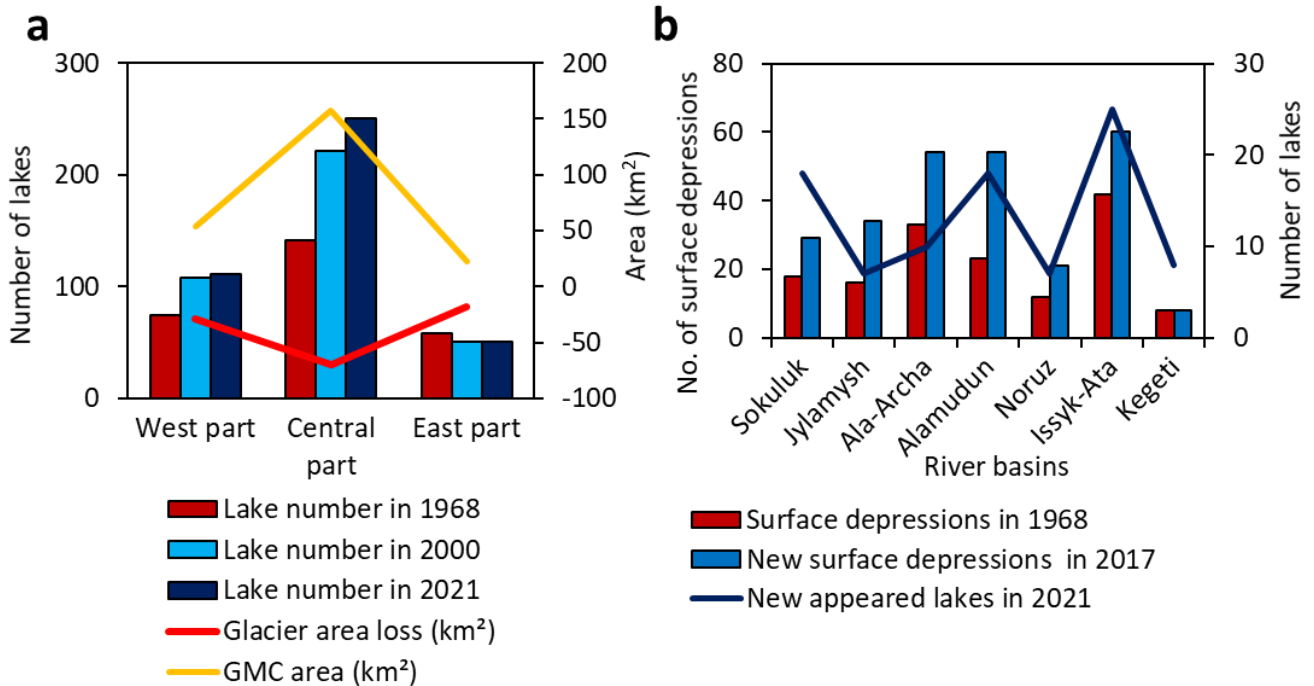
4.4 Differences in glacial lake patterns among river basins

Figure 8a 9a summarizes the evolution of lake numbers, glacier loss, and GMC area differs among the western, central, and eastern sectors-parts of the Kyrgyz Range (Fig. 9a), with boundaries shown in Fig. 1. In the western and central parts, While glacial lake the number of glacial lakes increased steadily in the western and central parts regions from 1968 to 2021, whereas a slight decrease in lake number was observed recorded in the eastern part. The highest concentration of both glacial lakes and GMCs is distributed in the central part of the range, where glacier loss is also greatest larger than others.

Focusing on individual catchments in the central part of the Kyrgyz Range (Fig. 8b9b), most newly formed appeared most glacial lakes are concentrated in the Issyk-Ata, Sokuluk, Ala-Archa, Alamudun, and Ala-Archa-Issyk-Ata basins, catchments. Repeated formation development of new surface depressions on GMCs, in the central part particularly in the Sokuluk, Jylamysh, Ala-Archa, Alamudun, Noruz, and Issyk-Ata river basins, is was associated with significant GMC surface changes and ongoing new lake development. In contrast, the Shamsy-North basin in the east and Ak-Suu basin in the western part have more than 30 lakes, while all other catchments have fewer than 30. This concentration of active GMC

370 evolution and thermokarst lake formation in the central part of the Kyrgyz Range points to it as a key zone for rapid glacial lake renewal and elevated future GLOF hazard potential.

highlights the central part of the Kyrgyz Range as a key area for both rapid GMC evolution and ongoing glacial lake formation, particularly thermokarst types engendered by accelerated buried ice melt.



375 **Figure 89:** a) Number of lakes in 1968, 2000, and 2021, and areas of glacier loss and GMCs in the three sections of the Kyrgyz Range. b) Number of surface depressions in 1968 and 2017, as well as new lakes formed between 2000 and 2021 in the central part of the range.

5 Discussion

380 5.1 Mechanisms underlying rapid glacial lake renewal

Between 2000 and 2021, 42% of the glacial lakes in the Kyrgyz Range were newly formed (Fig. 2), indicating highlighting an exceptionally dynamic lake system. This rapid turnover is consistent with observation mirrors trends observed in from the Kungoy and Ili Ranges of the northern Tien Shan (Narama et al., 2009). The primary dominant driver is glacier shrinkage: —glacier area has decreased by about approximately 3031% over the past five decades, and newly degraded deglaciated forefields force fields have developed into GMCs, greatly expanding. —As glaciers retreat, large portions of their forefields become GMCs, leading to the expansion of potential arcasites for lake formation (Fig. 5a).

385

The accelerated formation of contactless (thermokarst) lakes is further supported by the observed expansion and deepening of surface depressions (thermokarst features), resulting from the melting of buried ice within GMCs. ~~For example, At the Chelektor Glacier front, both downwasting and backwasting of buried ice have produced pronounced surface lowering and resulted in substantial morphological changes and the lateral enlargement~~ expansion of lake ~~basins~~ margins (Figs. 67, 78), ~~similar to. This mirrors~~ geomorphic processes observed on debris-covered glaciers elsewhere (Goldstein and Werner, 1997). Large depressions formed as a result of glacier surface downwasting, as ~~documented~~ reported for in the Teskey Range (Narama et al., 2010; Daiyrov et al., 2018), ~~subsequently filling~~ with meltwater and ~~evolve~~ transitioning into glacial lake.

~~In c~~Contrasting to the eastern Himalayas, where glacier-contact lakes often persist and gradually expand for decades (Yamada, 1998; Ageta et al., 2000; Iwata et al., 2002; Komori et al., 2004; Nagai et al., 2017), glacier retreat in the Kyrgyz Range has ~~mostly resulted in either~~ mainly led to the disappearance of contact lakes or their ~~transition~~ formation into contactless types (Fig. 4c). ~~As glacier upslope, Lakes former contact lakes by connected to glaciers become isolated and lose direct meltwater supply, which frequently as glaciers retreat upslope, no longer receiving direct meltwater input, which often~~ results in their eventual disappearance. The persistence and reappearance of contactless lakes ~~are~~ controlled by ~~linked to~~ local geomorphological conditions, ~~including such as~~ the existence of ice tunnels, buried ground ice, and the recurrent formation of surface depressions on GMCs. When meltwater or stream channels intersect these depressions, new thermokarst lakes can ~~repeatedly form, sometimes repeatedly~~ at the same location.

Recent climate warming has ~~increased~~ greatly enhanced the sensitivity of GMCs to melting, ~~accelerating~~ increasing rates of depression formation and ~~thereby~~ promoting additional enabling further glacial-lake development (Daiyrov et al., 2018; Daiyrov and Narama, 2021). ~~Consequently, Given these processes, GMCs must be should be recognized- regarded as key important~~ environments ~~for driving the~~ future growth/proliferation of contactless glacial lakes in the ~~Kyrgyz Range~~ region (Falatkova et al., 2019). ~~Notably, i~~n the Himalayas, lake development ~~is~~ remains more directly ~~associated~~ linked to with glacier shrinkage and the presence of large terminal moraines or ~~broad flat~~ outwash plains (Mool et al., 2001a; Iwata et al., 2002; Yamada, 1998; Javed et al., 2025). ~~Ahmed et al. (2021) reported that the expansion rates of pro-glacial lakes connected to glaciers and moraine-dammed lakes are faster than those of other types of lakes.~~ In contrast, the Kyrgyz Range ~~setting~~, with steep glacier forefields and ice-cored moraines, ~~favours~~ promotes more rapid, and recurrent ~~formation of~~ short-lived lakes, ~~a tendency-development-a trend that~~ likely to ~~intensify~~ accelerate further under continued warming and rising glacier equilibrium ~~line~~ altitudes (Marchenko et al., 2007; Niederer et al., 2008). ~~These features~~ highlights underscore the strong ~~control~~ influence of glacier retreat and subsequent GMC evolution on ~~the~~ dynamics of glacial lake formation and persistence ~~within~~ in the study region.

5.2 Regional variability in lake development

Glacial lake formation and turnover in the Kyrgyz Range ~~strongly exhibit concentrated pronounced spatial concentration~~ in the central basins of Sokuluk, Ala-Archa, Alamudun, and Issyk-Ata, where ~~the dense~~ density and expanding ~~of~~ GMCs ~~coincide with and~~ rapid glacier shrinkage, ~~leading to together foster~~ exceptionally high rates of lake appearance ~~dynamic lake~~

420 ~~emergence~~ and disappearance, and ~~elevated also increased~~ hazard potential. This central ~~partzone of the range~~ has also experienced ~~mostthe majority of~~ GLOF events over the past ~~two decades20 years~~ (Erokhin et al., 2017; Kattel et al., 2020; Daiyrov et al., 2022), ~~largely most~~ triggered by sudden drainage through ice tunnels within GMCs. ~~TheseSuch~~ processes are characterized by frequent depressions ~~formation~~ and subsequent thermokarst lake development, ~~reflecting the influence of~~ ~~directly linked to~~ ice-rich GMC morphology and the ablation of buried ice. Detailed DInSAR and UAV survey data ~~confirm~~
425 ~~corroborate this spatial variability, demonstrating~~ that rapid surface lowering ~~onwithin central area of the~~ GMCs ~~in the central part of the range drivesfosters~~ recurrent cycles of lake creation, ~~whereas~~. ~~By contrast~~, peripheral ~~river~~ basins ~~with characterized~~ by fewer or more stable GMCs ~~exhibit much more have shown relatively~~ limited changes in ~~theirglacial~~ lake systems.

~~Similar behaviorbehaviourComparable findings~~ have been reported ~~in~~ nearby regions of the northern Tien Shan. In the Teskey Range, thermokarst lakes ~~exhibit show~~ rapid fluctuations in surface area that are closely associated with GMC
430 conditions, ~~with short-term lake variability linked to persistent ablation of buried ice and frequent transitions among lake types~~ (Daiyrov et al., 2018; Daiyrov and Narama, 2021). ~~Short term variavilityvariability in glacial lakes has been attributed to persistent ablation of buried ice, resulting in rapid transitions in lake type.~~ ~~Short-livedterm lakes have been responsible for variations caused variability in lake type, and many of them changed under GMC change. Among these lake types, short lived type caused m~~most recent GLOFs in the Kyrgyz and Teskey Ranges, ~~where triggers often involve temporary closure and~~
435 ~~reopening of ice tunnels within GMCs~~ (Narama et al., 2010, 2018; Erokhin et al., 2017; Daiyrov et al., 2020, 2022). ~~Among these, short lived lakes have been responsible for most recent GLOFs in both the Kyrgyz and Teskey Ranges. The triggering mechanism for such events since 2000 has often been the temporary closure and reopening of ice tunnels within GMCs.~~ Tunnel blockage ~~maycan~~ result from debris deposition or ~~the~~ freezing of water ~~insidewithin~~ ice tunnels, ~~with debris frequently supplied by melting dead ice in GMCs~~ (Erokhin et al., 2012; Narama et al., 2018; ~~Daiyrov and Narama, 2021~~); ~~debris deposition is frequently linked to melting of dead ice within GMCs (Daiyrov et al., 2018; Daiyrov and Narama, 2021).~~ ~~The th~~Thawing of
440 buried ice through thermokarst processes leads to surface subsidence, collapse, and ~~the~~ subsequent formation of distinctive thermokarst lakes (Kääb and Haeberli, 2001). Thus, lake development in the Teskey Range ~~—and likewise in the Kyrgyz Range—~~ is ~~fundamentallystrongly~~ governed by GMC conditions and the presence of large volumes of buried ice.

Given ~~the continued rise inongoing~~ regional ~~warmingtemperatures~~, further melting of dead ice within GMCs is
445 ~~expectedanticipated~~, likely ~~causingresulting in~~ additional ~~depression~~ enlargement ~~of depressions~~, accelerated lake formation, and increased risk of sudden drainage events (GLOFs). Continuous monitoring and hazard assessment focus~~inged~~ on GMC-rich ~~chatchmentscatchmentsareas, particularalyparticularly—especially~~ those with population ~~areaseenters~~ downstream, ~~—are thus essential, even though this study does not explicitly therefore critical, even as this study does not directly~~ model future GLOF scenarios. ~~Nonetheless, our documentation of buried ice GMCs and rapidly evolving lakes offers an important~~
450 ~~foundation for anticipating and mitigating cryospheric hazards in the Kyrgyz Range.~~

At the ~~selalescale of broader~~ High Mountain Asia (HMA) ~~scale, glacial~~ lake expansion and ~~relatedGLOF~~ hazards are ~~being~~ increasingly recognized. Furian et al. (2022) projected the formation of large proglacial lakes across HMA through 2100. Recent studies demonstrated accelerated glacial lake growth and applied moraine-dam outburst models such as the eastern

Himalayas for GLOF risk assessment (Zhang et al., 2023; Chen et al., 2024). However, the processes of lake formation and GLOF triggering in the Tien Shan differ fundamentally from those in the eastern Himalayas. Therefore, effective assessment of disaster preparedness and future projections requires (1) current records of region-specific lake development and GLOF history, and (2) a detailed understanding of the characteristic lake formation processes specific to each mountain region.

6 Conclusions

This study quantifies the dynamic evolution of glacial lakes in the Kyrgyz Range, northern Tien Shan, over the period 1968–2021. During these 53 years, the number of glacial lakes increased from 274 in 1968 to 412 in 2021, ~~a nearly doubling,~~ while total lake area expanded by 76%, from 0.80 km² to 1.42 km². ~~Lake Turnover~~ was extremely high: of the 274 lakes present in 1968, 190 (69%) had disappeared by 2000. Despite these losses, 154 new lakes appeared by 2000, and 175 more had formed by 2021, with ~~just only~~ 84 lakes persisting ~~throughout across~~ the entire study period. Glacier area ~~simultaneously~~ shrank by ~~3231%~~ (from ~~390378.35~~ km² to ~~265262.40~~ km²), driving ~~the~~ widespread formation of ~~glacier moraine complexes~~ (GMCs) rich in buried ice. Surface lowering of ~~about up to~~ 5–30 m was observed in ~~4841%~~ of GMCs, and DInSAR analysis ~~revealed showed~~ that ~~7465%~~ of GMCs ~~exhibited showed~~ measurable deformation, ~~indicating active adjustment linked to buried-ice melt and favoring the rapid formation of new, often thermokarst, lakes. promoting the rapid development of new, often thermokarst lakes.~~ By 2021, over 70% of all glacial lakes were contactless types, reflecting the ~~pre~~dominance of lake formation ~~in~~ GMCs ~~rather than sustained over persistent~~ proglacial ~~lake~~ expansion. ~~These processes underpin a regime of constant glacial lake renewal, contrasting with the gradual expansion seen in the Himalayas.~~

In the Kyrgyz Range, glacial lakes renew rapidly due to the combination of accelerated glacier retreat, the expansion of glacier–moraine complexes (GMCs) containing buried ice, and ongoing climate warming. As glaciers shrink, newly exposed GMCs with significant dead ice melt and subside, forming new surface depressions that quickly fill with meltwater to create short-lived lakes. This geomorphological instability, coupled with repeated melting and reformation cycles, leads to a highly dynamic regime where glacial lakes frequently disappear, reappear, or form a new. The central ~~part of the~~ Kyrgyz Range, particularly the Sokuluk, Ala-Archa, and Issyk-Ata basins where many glaciers and GMCs are distributed, remains a hotspot for lake turnover and associated hazards. As warming continues, monitoring lake dynamics and GMC changes will be vital for hazard assessment and adaptation in the region. ~~Integrating DInSAR with optical inventories and field validation remains essential. These findings demonstrate that glacial lakes in the Kyrgyz Range are characterized by continual renewal, driven by the combined effects of accelerated glacier retreat, GMC expansion and degradation, and ongoing climate warming, and that this regime contrasts sharply with the more gradual, persistent lake growth observed in regions such as the eastern Himalayas.~~

Funding

Grant-in-Aid for Scientific Research (B) (19H01372 and 23K22023) of MEXT KAKENHI Grant.

485

Acknowledgments

We thank two reviewers for their valuable comments and suggestions. This work was supported by Grant-in-Aid for JSPS Fellows (22F22006) of JSPS KAKENHI Grant and Grant-in-Aid for Scientific Research (B) (19H01372 and 23K22023) of MEXT KAKENHI Grant. This study used ALOS satellite image data from ALOS Research Announcement (RA) in the framework of JAXA EORC.

References

- Ahmed, R., Wani, G. F., Ahmad, S. T., Sahana, M., Singh, H., and Ahmed, P.: A review of glacial lake expansion and associated glacial lake outburst floods in the Himalayan region. *Earth Systems and Environment*, 5(3), 695-708, 2021.
- Agarwal, V., Wyk de Vries, M. V., Haritashya, U. K., Garg, S., Kargel, J. S., Chen, Y., and Shugar, D. H.: Long-term analysis of glaciers and glacier lakes in the Central and Eastern Himalaya, *Sci. Total Environ.*, 898, 165598, <https://doi.org/10.1016/j.scitotenv.2023.165598>, 2023.
- Ageta, Y., Iwata, S., Yabuki, H., Naito, N., Sakai, A., Narama, C., and Karma.: Expansion of glacier lakes in recent decades in the Bhutan Himalayas, in: IAHS Publ., Wallingford, UK, 165–175, 2000.
- Aizen, V. B., Aizen, E. M., and Melack, J. M.: Climate and hydrologic changes in the Tien Shan, central Asia, *J. Climate*, 10, 1393–1404, 1997.
- Aizen, V. B., Kuzmichenok, V. A., Surazakov, A. B., and Aizen, E. M.: Glacier changes in the central and northern Tien Shan during the last 140 years based on surface and remote-sensing data, *Ann. Glaciol.*, 43, 202–213, <https://doi.org/10.3189/172756406781812465>, 2006.
- Azisov, E., Hoelzle, M., Vorogushyn, S., Saks, T., Usubaliyev, R., Esenaman uulu, M., and Barandun, M.: Reconstructed centennial mass balance change for Golubin Glacier, northern Tien Shan, *Atmosphere*, 13, 954, <https://doi.org/10.3390/atmos13060954>, 2022.
- Atwood, D. K., Meyer, F., and Arendt, A.: Using L-band SAR coherence to delineate glacier extent. *Can. J. Remote Sensing*, Vol. 36, Suppl. 1, pp. S186–S195, 2010.
- Blöthe, J. H., Halla, C., Schwalbe, E., Bottegal, E., Liaudat, D. T., and Schrott, L.: Surface velocity fields of active rock glaciers and ice-debris complexes in the Central Andes of Argentina, *Earth Surf. Process. Landf.*, 46, 504–522, <https://doi.org/10.1002/esp.5042>, 2021.
- Bolch, T.: Climate change and glacier retreat in northern Tien Shan (Kazakhstan/Kyrgyzstan) using remote sensing data, *Glob. Planet. Change*, 56, 1–12, <https://doi.org/10.1016/j.gloplacha.2006.07.009>, 2007.
- Bolch, T.: Glacier area and mass changes since 1964 in the Ala-Archa Valley, Kyrgyz Ala-Too, northern Tien-Shan, *Ice Snow*, 129, 28–39, <https://doi.org/10.15356/IS.2015.01.03>, 2015.

- Bolch, T., Rohrbach, N., Kutuzov, S., Robson, B. A., and Osmonov, A.: Occurrence, evolution and ice content of ice-debris complexes in the Ak-Shiirak, Central Tien Shan revealed by geophysical and remotely-sensed investigations, *Earth Surf. Process. Landf.*, 44, 129–143, <https://doi.org/10.1002/esp.4487>, 2019.
- 520 [Buchelt, S., Kunz, J., Wiegand, T., and Kneisel, C.: Dynamics and internal structure of a rock glacier: Inferring relationships from the combined use of differential synthetic aperture radar interferometry, electrical resistivity tomography and ground-penetrating radar. *Earth Surface Processes and Landforms*, 49\(14\), 4743–4758, <https://doi.org/10.1002/esp.5993>, 2024.](#)
- [Buckel, J., Otto, J. C., Prasicek, G., Keuschnig, M.: Glacial lakes in Austria - Distribution and formation since the Little Ice Age. *Glob. Planet. Change*, 164, 39–51, <https://doi.org/10.1016/j.gloplacha.2018.03.003>, 2018.](#)
- 525 Chen, M., Chen, Y., Fang, G., Zheng, G., Li, Z., and Li, Y.: Risk assessment of glacial lake outburst flood in the Central Asian Tianshan Mountains, *Clim. Atmos. Sci.*, 7, 209, <https://doi.org/10.1038/s41612-024-00755-6>, 2024.
- Daiyrov, M., Narama, C., Yamanokuchi, T., Tadono, T., Kääh, A., and Ukita, J.: Regional geomorphological conditions related to recent changes of glacial lakes in the Issyk-Kul basin, northern Tien Shan, *Geosciences*, 8, 99, <https://doi.org/10.3390/geosciences8030099>, 2018.
- 530 Daiyrov, M., Narama, C., Kääh, A., and Tadono, T.: Formation and outburst of Toguz-Bulak glacial lake in the north part of Teskey Range, Tien Shan, Kyrgyzstan, *Geosciences*, 10, 468, <https://doi.org/10.3390/geosciences10110468>, 2020.
- Daiyrov, M., Kattel, D. B., Narama, C., and Wang, W.: Evaluating the variability of glacial lakes in the Kyrgyz and Teskey Ranges, Tien Shan, *Front. Earth Sci.*, 14, 112–119, 2022.
- Daiyrov, M., and Narama, C.: Formation, evolution, and drainage of short-lived glacial lakes in permafrost environments of the northern Teskey Range, Central Asia, *Nat. Hazards Earth Syst. Sci.*, 21, 2245–2256, <https://doi.org/10.5194/nhess-21-2245-2021>, 2021.
- 535 Erokhin, S.: Data report of glacial lakes in 2000–2008, in: *Inventory of Glacial Lakes*, Ministry of Emergency Situations of the Kyrgyz Republic, Bishkek, (in Russian), 2008.
- Erokhin, S.: Types of moraine complexes and Tien-Shan glaciation, *Izvestiya NAS KR*, Bishkek, 115–118 (in Russian), 2011.
- 540 Erokhin, S., Zaginaev, V., Meleshko, A., Ruiz-Villanueva, V., Petrakov, D. A., and Chernomorets, S. S.: Debris flows triggered from nonstationary glacier lake outbursts: The case of the Teztor Lake complex (Northern Tian Shan, Kyrgyzstan), *Landslides*, 15, 83–98, <https://doi.org/10.1007/s10346-017-0862-3>, 2017.
- Falatkova, K., Šobr, M., Neureiter, A., Schöner, W., Janský, B., Häusler, H., Engel, Z., and Beneš, V.: Development of proglacial lakes and evaluation of related outburst susceptibility at the Adygin ice-debris complex, northern Tien Shan, *Earth Surf. Dynam.*, 7, 301–320, <https://doi.org/10.5194/esurf-7-301-2019>, 2019.
- 545 Furian, W., Maussion, F., and Schneider, C.: Projected 21st-century glacial lake evolution in high mountain Asia, *Front. Earth Sci.*, 10, 821798, <https://doi.org/10.3389/feart.2022.821798>, 2022.
- Goldstein, R. M., and Werner, C. L.: Radar ice motion interferometry, in: *Proc. 3rd ERS ESA Symp.*, ESA SP, Florence, Italy, 969–972, 1997.

- 550 Goldstein, R. M., and Werner, C. L.: Radar interferogram phase filtering for geophysical applications, *Geophys. Res. Lett.*, 25, 4035–4038, 1998.
- Hanshaw, M. N., and Bookhagen, B.: Glacial areas, lake areas, and snow lines from 1975 to 2012: Status of the Cordillera Vilcanota, including the Quelccaya ice cap, northern central Andes, Peru, *Cryosphere*, 8, 359–376, <https://doi.org/10.5194/tc-8-359-2014>, 2014.
- 555 [Izagirre, E., Casassa, G., Dussailant, I., Miles, E. S., Wilson, R., Rada, C., Faria, S. H., and Antiguiedad, I.: Evolution of glacial lakes and southernmost GLOFs in the Cordillera Darwin and Cloue Icefields \(Tierra del Fuego\) between 1945–2024. *Front. Earth Sci.* 13:1641167. doi: 10.3389/feart.2025.1641167, 2025.](#)
- Iwata, S., Ageta, Y., Sakai, A., Narama, C., and Karma.: Glacial lakes and their outburst flood assessment in the Bhutan Himalaya, *Glob. Environ. Res.*, 6, 3–17, 2002.
- 560 Janský, B., Šobr, M., and Erokhin, S. A.: Typology of high mountain lakes of Kyrgyzstan with regard to the risk of their rupture, *Limnol. Rev.*, 6, 135–140, 2006.
- Janský, B., Šobr, M., and Engel, Z., and Yerokhin, S.: High-altitude lake outburst: Tien-Shan case study, in: Dostál, P. (Ed.), *Evolution of geographical systems and risk processes in the global context*, Charles Univ. Prague, Faculty of Science, P3K Publishers, Prague, 113–127, 2008.
- 565 Janský, B., Šobr, M., and Engel, Z.: Outburst flood hazard: Case studies from the Tien-Shan Mountains, Kyrgyzstan, *Limnol-Ecol. Manage. Inland Waters*, 40, 358–364, 2010.
- [Javed, M., Böhner, J., Hasson, S.: Mapping Glacial Lakes in the Western Himalayas Using an Enhanced Breakpoint Method and CubeSat Imagery. *PFG – Journal of Photogrammetry, Remote Sens. and Geoinf. Science*, 93, 401–419, 2025.](#)
- Kääb, A., and Haeberli, W.: Evolution of a high-mountain thermokarst lake in the Swiss Alps, *Arct. Antarct. Alp. Res.*, 33, 385–390, <https://doi.org/10.1080/15230430.2001.12003445>, 2001.
- 570 Kattel, D. B., Mohanty, A., Daiyrov, M., Wang, W., Mishra, M., Kulenbekov, Z., and Dawadi, B.: Evaluation of glacial lakes and catastrophic floods on the northern slopes of the Kyrgyz Range, *MRD*, 40, 3, <https://doi.org/10.1659/MRD-JOURNAL-D-19-00068.1>, 2020.
- Komori, J., Gurung, D. R., Iwata, S., and Yabuki, H.: Variation and lake expansion of Chubda Glacier, Bhutan Himalayas, during the last 35 years, *Bull. Glaciol. Res.*, 21, 49–55, <https://doi.org/10.5331/bgr.21.49>, 2004.
- 575 [Kunz, J., Ullmann, T., Kneisel, C.: Internal structure and recent dynamics of a moraine complex in an alpine glacier forefield revealed by geophysical surveying and Sentinel-1 InSAR time series. *Geomorphology*, 398, 108052, <https://doi.org/10.1016/j.geomorph.2021.108052>, 2022.](#)
- 580 [Kunz, J., Buchelt, S., Wiegand, T., Ullmann, T., Kneisel, C.: Thrust moraines and rock glaciers: Relationships between subsurface structures and morphodynamics in Swiss glacier forefields dominated by glacier-permafrost interactions. *Cop. Publ.* <https://doi.org/10.5194/egusphere-2025-1671>, 2025. \(Preprint\).](#)
- Maksimov, E. V.: Climate Change and Mountain Glaciation in the New Era, *Proc. Russian Geogr. Soc.*, 114, 2, 1982.

- Maksimov, E. V., and Osmonov, A. O.: Features of modern glaciation and glacier dynamics of the Kyrgyz Ala-Too, Natl. Acad. Sci. Kyrgyz Rep., Tian Shan Phys.-Geogr. Stn. Inst. Geol., Bishkek, Ilim, 200 pp., ISBN 5-8355-0845-X, 1995.
- 585 Marchenko, S. S., Gorbunov, A. P., and Romanovsky, V. E.: Permafrost warming in the Tien Shan Mountains, Central Asia, *Glob. Planet. Change*, 56, 311–327, <https://doi.org/10.1016/j.gloplacha.2006.07.023>, 2007.
- Mool, P. K., Bajracharya, S. R., and Joshi, S. P.: Inventory of Glaciers, Glacial Lakes and Glacial Lake Outburst Floods, Monitoring and Early Warning Systems in the Hindu Kush-Himalayan Region: Nepal, ICIMOD & UNEP RRC-AP, 2001.
- 590 Nagai, H., Ukita, J., Narama, C., Fujita, K., Sakai, A., and Tadono, T.: Evaluating the scale and potential of GLOF in the Bhutan Himalayas using a satellite-based integral glacier-glacial lake inventory, *Geosciences*, 7, 77, <https://doi.org/10.3390/geosciences7030077>, 2017.
- Narama, C., Severskiy, I., and Yegorov, A.: Current state of glacier changes, glacial lakes, and outburst floods in the Ile Ala-Tau and Kungöy Ala-Too ranges, northern Tien Shan Mountains, *Ann. Hokkaido Geogr.*, 84, 22–32, <https://doi.org/10.14943/geoexp.84.22>, 2009.
- 595 [Narama, C., Daiyrov, M., Tadono, T., Yamamoto, M., Kääb, A., Morita, R., Ukita, J.: Seasonal drainage of supraglacial lakes on debris-covered glaciers in the Tien Shan Mountains, Central Asia. *Geomorphology*, 286, 133-142, 2017.](#)
- Narama, C., Duishonakunov, M., Kääb, A., Daiyrov, M., and Abdrakhmatov, K.: The 24 July 2008 outburst flood at the western Zyndan glacier lake and recent regional changes in glacier lakes of the Teskey Ala-Too range, Tien Shan, Kyrgyzstan, *Nat. Hazards Earth Syst. Sci.*, 10, 647–659, <https://doi.org/10.5194/nhess-10-647-2010>, 2010.
- 600 Narama, C., Daiyrov, M., Duishonakunov, M., Tadono, T., Sato, H., Kääb, A., Ukita, J., and Abdrakhmatov, K.: Large drainages from short-lived glacial lakes in the Teskey Range, Tien Shan Mountains, Central Asia, *Nat. Hazards Earth Syst. Sci.*, 18, 983–995, <https://doi.org/10.5194/nhess-18-983-2018>, 2018.
- Niederer, P., Bilenko, V., Ershova, N., Hurni, H., Yerokhin, S., and Maselli, D.: Tracing glacier wastage in the Northern Tien Shan (Kyrgyzstan/Central Asia) over the last 40 years, *Climatic Change*, 86, 227–234, <https://doi.org/10.1007/s10584-007-9288-6>, 2008.
- 605 Ponomarenko, P. N.: Atmospheric precipitation of Kyrgyzstan, Hydrometeo Publ. House, Leningrad, 134 pp., 1976.
- Quincey, D. J., Richardson, S. D., Luckman, A., Lucas, R. M., Reynolds, J. M., Hambrey, M. J., and Glasser, N. F.: Early recognition of glacial lake hazards in the Himalaya using remote sensing datasets, *Glob. Planet. Change*, 56, 137–152, 2007.
- 610 [Sakurai, N., Narama, C., Daiyrov, M., Esenamanov, M., Usekov, Z., Inoue, H.: Simultaneous drainage events from supraglacial lakes on the southern Inylchek Glacier, Central Asia. *Journal of Glaciology*, 1-12, 2021.](#)
- [Sandwell, D. T., Myer, D., Mellors, R., Shimada, M., Brooks, B., and Foster, J.: Accuracy and resolution of ALOS interferometry: Vector deformation maps of the Father's Day intrusion at Kilauea, *IEEE Trans. Geosci. Remote Sens.*, 46, 3524–3534, <https://doi.org/10.1109/TGRS.2008.2000634>, 2008.](#)
- 615 Shatravin, V. I., and Stavitski, J. S.: Methodological bases for the identification of settling factors during detailed studies of high-altitude lakes, *Selevye Potoki, Hydrometeorol. Publ. House*, 83–92, 1984.

- Shatravin, V. I.: Reconstruction of Pleistocene and Holocene glaciations in the Tien-Shan from new starting positions, in: *Climate, Glaciers and Lakes: Journey to the Past*, Ilim, Bishkek, 26–46, 2007.
- 620 ~~Sandwell, D. T., Myer, D., Mellers, R., Shimada, M., Brooks, B., and Foster, J.: Accuracy and resolution of ALOS interferometry: Vector deformation maps of the Father's Day intrusion at Kilauea, *IEEE Trans. Geosci. Remote Sens.*, 46, 3524–3534, <https://doi.org/10.1109/TGRS.2008.2000634>, 2008.~~
- Strozzi, T., Kääb, A., and Frauenfelder, R.: Detecting and quantifying mountain permafrost creep from in situ inventory, space-borne radar interferometry and airborne digital photogrammetry, *Int. J. Remote Sens.*, 25, 2919–2931, <https://doi.org/10.1080/0143116042000192330>, 2004.
- 625 Usubaliev, R., and Erokhin, S.: Formation of high-mountainous lakes as a consequence of the degradation of the modern glaciation of the Tien Shan, in: *Data of Glaciological Studies*, NAS KR, Bishkek, 134–137, 2007.
- Werner, C., Wegmüller, U., Strozzi, T., and Wiesmann, A.: Gamma SAR and interferometric processing software, in: Sawaya-Lacoste, H. (Ed.), *ERS-ENVISAT Symp.*, Gothenburg, Sweden, ESA Publ. Div., Noordwijk, 2000.
- 630 Yamada, T.: Glacier lake and its outburst flood in the Nepal Himalaya, *Data Center for Glacier Research*, Japanese Society of Snow and Ice, Monograph No. 1, Tokyo, 1998.
- Zaginaev, V., Ballesteros-Cánovas, J., Matov, E., Petrakov, D., and Stoffel, M.: Reconstruction of glacial lake outburst floods in northern Tien-Shan: Implications for hazard assessment, *Geomorphology*, 269, 75–84, <https://doi.org/10.1016/j.geomorph.2016.06.028>, 2016.
- Zaginaev, V., Falatkova, K., Jansky, B., Sobr, M., and Erokhin, S.: Development of a potentially hazardous pro-glacial lake 635 in Aksay valley, Kyrgyz Range, northern Tien Shan, *Hydrology*, 6, 3, <https://doi.org/10.3390/hydrology6010003>, 2019.
- Zhang, T., Wang, W., An, B., and Wei, L.: Enhanced glacial lake activity threatens numerous communities and infrastructure in the Third Pole, *Nat. Commun.*, 14, 8250, <https://doi.org/10.1038/s41467-023-44123-z>, 2023.